

上扬子会泽地区早三叠世飞仙关组砂岩物源特征： 来自重矿物铬尖晶石和碎屑锆石的限定

张英利¹⁾, 王宗起¹⁾, 王刚¹⁾, 李谦²⁾, 林健飞³⁾

1) 中国地质科学院矿产资源研究所, 国土资源部成矿作用与矿产资源评价重点实验室, 北京, 100037;
2) 中国石油勘探开发研究院, 北京, 100083;
3) 中国地质大学(北京), 北京, 100083

内容提要: 上扬子会泽地区早三叠世飞仙关组主要为河流相的紫红色砂岩, 物源主要来自于西部和西北部。碎屑重矿物组合表明物源主要来自于岩浆岩, 且重矿物中发现大量碎屑铬尖晶石和锆石。本文运用电子探针微区成分分析和碎屑锆石 U-Pb 测年方法, 对上扬子早三叠世飞仙关组砂岩中铬尖晶石和碎屑锆石进行分析。铬尖晶石电子探针化学成分分析显示, 其具有高铬、低 Fe^{3+} 和高 TiO_2 含量的特征, 源岩分析指示这些铬尖晶石来源于与洋岛/板内、岛弧以及大火成岩省相关的火成岩。同时, 碎屑锆石 LA-ICP-MS U-Pb 年龄测定表明, 飞仙关组的物源主要来自于 248 ~ 272 Ma 和 715 ~ 997 Ma 的岩浆岩。铬尖晶石和碎屑锆石综合分析表明, 248 ~ 272 Ma 的物源岩石具有大火成岩省玄武岩特征, 主要为峨眉山玄武岩及同期基性侵入岩; 715 ~ 997 Ma 的物源为洋岛/板内玄武岩类, 主要为研究区周缘与新元古代苏雄组及其同期的岩浆岩; 铬尖晶石指示的岛弧性质物源则可能源自 1000 ~ 1100 Ma 的岩浆岩。同时, 碎屑锆石还指示古元古代和早寒武世发育岩浆作用, 且存在古老的新太古代结晶基底。这些资料为上扬子地区构造演化提供了沉积学的证据。

关键词: 上扬子; 碎屑重矿物; 铬尖晶石; 碎屑锆石年代学; 物源分析

碎屑岩地球化学较成功地将主量元素、微量元素和稀土元素的特征运用于母岩类型、构造背景等分析, 得到了大家的广泛应用 (Bhatia, 1983; Roser and Korsch, 1988; Jorge et al., 2013), 但在使用过程中存在一定的局限性 (Armstrong-Altrin and Verma, 2005; Ryan and Williams, 2007)。而碎屑重矿物(例如铬尖晶石)由于稳定性强、受后期的影响较少, 很好的诠释沉积盆地中陆源碎屑沉积的古地理、构造背景等, 成为比碎屑岩地球化学更有效的方法之一 (Cookenboo et al., 1997; Lee, 1999; Lenaz et al., 2009)。同时, 碎屑锆石能够更好限定源区岩石形成年龄或变质结晶年龄, 而且可用来进行区域岩石—构造单元对比、古地理格局恢复 (Fedo et al., 2003; Leier et al., 2007; Gehrels, 2012), 也成为物源分析的重要手段。

前人沉积学研究结果表明, 上扬子地区飞仙关组沉积物形成于河流环境 (唐勇等, 2007)、冲积

扇—河口湾环境 (赵玉光等, 1996)、碳酸盐台地环境 (田景春等, 2000; 肖加飞等, 2004), 而上扬子地区 (研究区北部) 飞仙关组的纹层状微晶灰岩、灰质页岩或条带状灰岩代表了古特提斯海海洋循环的近乎停滞的低能环境 (时志强等, 2010)。因此, 飞仙关组沉积时期, 不同地区的沉积环境和岩相古地理存在差异。然而, 对于飞仙关组碎屑岩的母岩特征及物源研究则甚少, 制约了上扬子地区三叠纪的构造—沉积演化过程研究。会泽地区处于上扬子地区盆山结合部, 三叠纪露头连续, 尤其是早三叠世飞仙关组以碎屑岩为主, 沉积序列清晰, 真实记录了其演化过程, 是研究上扬子地区碎屑物源及演化的理想区域。

本文通过对会泽地区飞仙关组的野外地质调查, 分析重矿物组成, 分别对单矿物铬尖晶石和碎屑锆石进行电子探针和 LA-ICP-MS U-Pb 测年分析, 探讨飞仙关组物源的构造背景以及物源区特征, 为上

注: 本文为国家自然基金(编号:41302080)和中国地质调查局地质调查项目(编号:12120114009401)资助成果。

收稿日期: 2014-09-14; 改回日期: 2015-10-10; 责任编辑: 黄敏。Doi: 10.16509/j.georeview.2016.01.005

作者简介: 张英利, 男, 1979 年生。博士, 副研究员, 主要从事盆地构造与沉积学研究。通讯地址: 100037, 中国地质科学院矿产资源研究所。Email: yinglizh@126.com。

扬子地区构造演化提供进一步依据。

1 区域地质背景

上扬子地区受中—新生代构造运动的影响,分别以重要的断裂(龙门山断裂、鲜水河断裂、小江断裂等)为界,由盐源褶冲带、松潘—甘孜造山带、龙门山造山带和四川盆地等不同的构造单元组成(图1)。

1.8~1.6 Ga时期,受哥伦比亚超大陆裂解作用影响,扬子陆块西缘龙门山—安宁河断裂东侧发育被动大陆边缘裂谷系(尹福光等,2012a),同时大量辉长岩、辉绿岩等侵入(Zhao Xinfu et al., 2010; 王冬兵等,2013; 王正等,2013; 郭阳等,2014);新元古代时期受Rodinia超大陆裂解(Li et al., 2002; 崔晓庄等,2012; 任光明等,2013; 程佳孝等,2014)或者板

块俯冲作用(Zhou et al., 2007; Zhao Junhong et al., 2007)影响,形成分布广泛的830~795 Ma和780~745 Ma岩浆岩,从龙门山向西南经康定再向南经过石棉、冕宁、米易至攀枝花和元谋(研究区西南),主要岩性包括闪长岩、花岗岩、辉长岩和镁铁—超镁铁质岩,与此同时发育以碎屑沉积为主的裂谷盆地(王剑等,2001);新元古代晚期至早奥陶世,研究区进入稳定的发展阶段(黄福喜等,2011),主要以碳酸盐沉积为主;中奥陶世—志留纪,受挤压作用影响,边缘隆升;泥盆纪—中三叠世,以伸展作用为主,发育裂陷和坳陷盆地(陈洪德等,2011),尤其是晚二叠世,受地幔柱活动影响,形成以玄武岩为主的峨眉山大火成岩省(LIP)(Fan Weiming et al., 2004; Zhong Hong et al., 2007; Shellnutt et al., 2008; Xu Yigang et al., 2008),分布于川西、滇、黔西等地区;

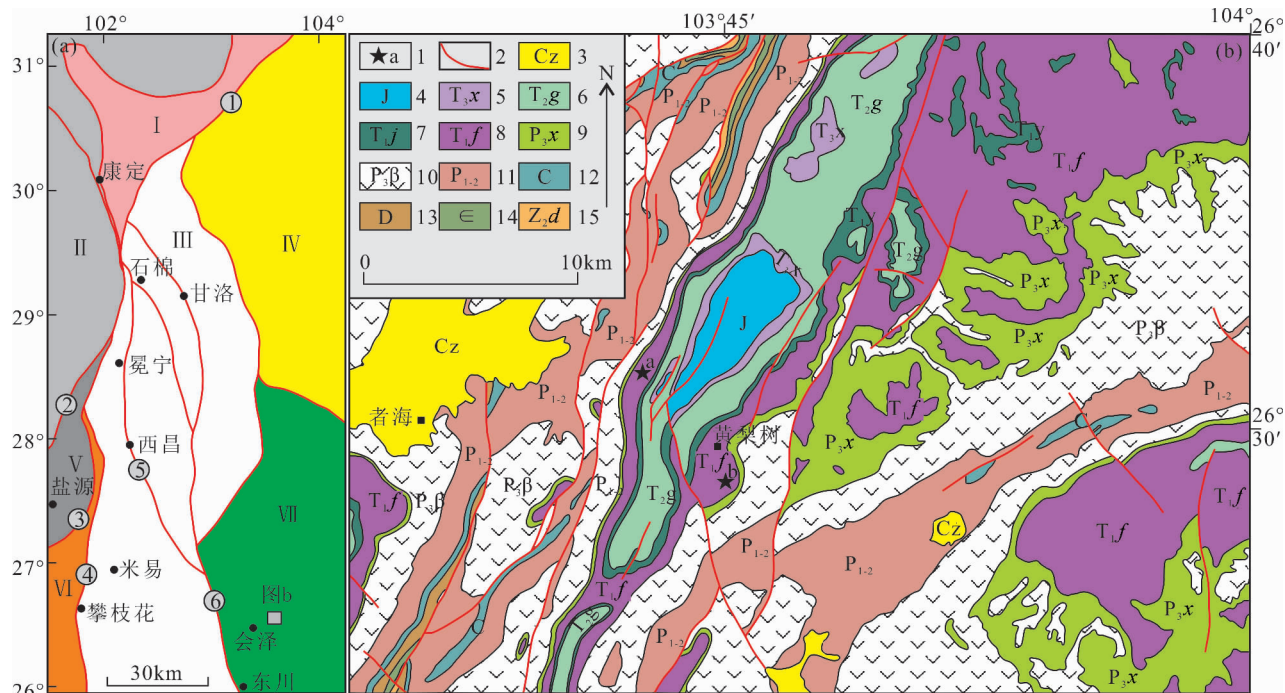


图1 大地构造单元图(a)和会泽地区地质图(b,据1:20万东川幅地质图^①修改)

Fig. 1 Tectonic units division (a) and simplified geological map of Huize area (b, modified from the

1/200 000 Regional Geological Report of Dongchuan Area^①)

(a) 构造分区: I—龙门山造山带; II—松潘—甘孜造山带; III—康滇古陆; IV—四川盆地; V—盐源褶冲带; VI—楚雄盆地; VII—滇东台褶带。断裂:①—龙门山断裂;②—金河断裂;③—箐河断裂;④—鲜水河断裂;⑤—则木河断裂;⑥—小江断裂。

(b) 地质图:1—剖面位置和取样位置;2—断层;3—新生界;4—侏罗系;5—须家河组;6—关岭组;7—嘉陵江组;8—飞仙关组;9—宣威组;10—峨眉山玄武岩;11—二叠系中一下统;12—石炭系;13—泥盆系;14—寒武系;15—灯影组

(a) Tectonic units: I—Longmenshan orogenic belt; II—Songpan—Ganzi orogenic belt; III—Kangdian Oldland; IV—Sichuan basin; V—Yanyuan fold and thrust belt; VI—Chuxiong basin; VII—Eastern Yunnan platform fold belt. Fault: ①—Longmenshan fault; ②—Jinhe fault; ③—Qinghe fault; ④—Xianshuihe fault; ⑤—Zemuhe fault; ⑥—Xiaojiang fault.

(b) Geological map: 1—Sample location; 2—fault; 3—Cenozoic; 4—Jurassic; 5—Xujiahe Formation; 6—Guanling Formation; 7—Jialingjiang Formation; 8—Feixianguan Formation; 9—Xuanwei Formation; 10—Emeishan Basalt; 11—Lower—Middle Permian; 12—Carboniferous; 13—Devonian; 14—Cambrian; 15—Dengying Formation.

晚三叠世之后,随着海水的逐渐退却和陆内碰撞造山作用,形成了以须家河组陆相碎屑沉积为代表的前陆盆地(林良彪等,2006;郑荣才等,2011;Deng et al., 2012)。

本次研究的主要地区——会泽地区属于上扬子滇东台褶带,虽然受不同时期构造事件影响,但研究区地层出露较完整(图1和2)。新元古界主要为灯影组含藻白云岩和白云岩,赋存大量铅锌矿(李文博等,2006),寒武系主要是潮坪相砂岩,局部夹白云岩;研究区缺失奥陶系和志留系,寒武系直接被泥盆纪砂岩所覆盖。早—中二叠世主要为生物碎屑灰岩,晚二叠世主要出露峨眉山玄武岩和宣威组碎屑岩。玄武岩主要分布中南部和西北部,而宣威组碎屑岩与玄武岩同期异相(许连忠等,2006),形成于

海陆过渡环境(邵龙义等,2013),分布于研究区东部。研究区三叠纪主要划分为飞仙关组、嘉陵江组、关岭组(与雷口坡组同期)和须家河组(图2)。飞仙关组主要是灰紫色砂岩夹粉砂岩,局部见灰岩;嘉陵江组整合覆盖于飞仙关组之上,下部主要为灰绿色砂岩,局部夹紫红色细砂岩,上部为浅灰色灰岩;关岭组主要为紫红色砂岩和粉砂岩互层,上部主要为灰岩和白云岩;晚三叠世须家河组沉积了冲积环境的灰黄色砂岩和泥岩,其与下伏关岭组为平行不整合接触。侏罗系和新生界主要为紫红色、土黄色的砂砾岩等。

2 沉积学特征

本次研究分别对研究区内南北两侧出露的飞仙

界	系	统	组	岩性	描 述
新生界	第四系	更新统			浅黄色、土黄色泥砾岩和灰色粘土
	侏罗系				下部为紫红、灰黄、灰绿色粉砂质泥岩、粉砂岩, 中部为紫红色粉砂岩与细砂岩互层, 上部为紫红色、灰绿色泥岩
中生界	三叠系	上	须家河组 T ₃ x		下部为灰黄、灰白色中砂岩, 上部为灰黄色细砂岩与泥岩互层
		中	关岭组 T ₂ g		下部为紫红、灰黄色细-中砂岩、粉砂岩互层, 夹灰黑色灰岩, 上部为浅灰色粉砂质灰岩和白云岩
		下	嘉陵江组 T ₁ y		下部为灰黄、灰绿色中-细砂岩夹紫红色细砂岩及黄绿色泥岩, 上部为灰、浅灰色灰岩, 夹浅棕红、黄绿色泥岩
			飞仙关组 T ₁ f		下部为灰紫色砂岩夹粉砂岩, 上部为紫红色泥质粉砂岩、粉砂质泥岩, 夹灰紫色细砂岩。局部见浅灰色灰岩
	二叠系	上	宣威组 P ₃ x	玄武岩 P ₃ β	灰黄、黄绿色粉砂岩、细砂岩和泥岩 暗绿、深灰色玄武岩、杏仁玄武岩, 夹玄武岩质火山角砾岩
		中下	P ₁₋₂		灰、浅灰色灰岩、白云质灰岩夹白云岩, 见硅质结核, 顶部为生物碎屑灰岩
古生界	石炭系		C		下部为灰色、深灰色灰岩夹白云岩, 上部为浅灰色、灰白色白云岩
	泥盆系		D		下部为紫红色中-细砂岩夹灰黑色灰岩, 上部为灰色、浅灰色黄灰色白云岩
	寒武系		Є		下部为灰绿色粉砂岩、细砂岩夹灰色白云岩, 上部为浅灰色白云岩
新元古界	灯影组Z ₂ d				灰、灰白色含藻白云岩和白云岩

图 2 会泽地区地层格架(资料来源:张远志,1996;辜学达等,1997)

Fig. 2 Stratigraphy framework in the Huize area, Upper Yangtze
(According to: Zhang Yuanzhi, 1996#; Gu Xueda et al., 1997#)

关组进行野外地质调查。沉积序列表明,北侧飞仙关组主要为紫红色中—粗砂岩与紫红色薄层泥岩(图3a),砂岩发育大型板状交错层理(图4a)和平行层理,砂岩呈透镜状,局部含有少量次圆状泥岩砾石(图4b),砾石排列与分布无规律。南侧飞仙关组下部为紫红色粗砂岩和紫红色泥岩(图3b),粗砂岩发育板状交错层理,可见泥砾。泥岩中发育砂岩透镜体;上部为紫红色泥岩、粉砂岩(图4c)与紫红色细砂岩。砂岩和粉砂岩发育交错层理(图4d),粉砂岩、泥岩中夹透镜状细砂岩。综合分析说明,飞仙关组形成于辫状河环境(Nemec et al., 1984),含砾粗砂岩、中—粗砂岩为河道滞留沉积,紫红色粉砂岩、泥岩是河道泛滥或者洪水决口时的泛滥平原或决口扇沉积。板状交错层理恢复的古流向表明沉积物源主要来自于西部和西北部(图3)。

野外和显微镜下观察表明,飞仙关组砂岩分选较差,磨圆较好,为次棱角—圆状;杂基含量较少,主要为颗粒支撑,少量基质支撑的砂岩后期发生碳酸盐交代作用。砂岩颗粒主要由石英和岩屑组成,其中岩屑颗粒主要为火山岩和硅质岩岩屑,变质岩岩屑相对较少。

3 重矿物分析

样品10HLS2和10HLS16采自会泽黄梨树飞仙关组(图1),采样位置分别为 $(26^{\circ}31'29'', 103^{\circ}42'41'')$ 和 $(26^{\circ}29'39'', 103^{\circ}45'11'')$,样品重量约10kg。重砂分析在河北省区域地质矿产调查研究所实验室完成。飞仙关组砂岩内主要识别出锆石、磷灰石、辉石、铬铁矿、赤—褐铁矿、磁铁矿等重矿物(表1)。重矿物中以赤—褐铁矿的含量最多,磁铁矿次之,赤铁矿、褐铁矿可能为黄铁矿氧化而来,对于物源指示没有实际意义。除赤—褐铁矿之外,磷灰石+白钛石+辉石+铬铁矿+磁铁矿组合说明物源来自于岩浆岩,部分磷灰石可能来自于变质岩。碎屑重矿物表明,2个样品的物源区存在少量差异。挑选样品10HLS2重矿物中的铬尖晶石和锆石,便于进行后续的电子探针分析和LA-ICP-MS U-Pb年龄测试。

表1 会泽地区飞仙关组砂岩重矿物组成(%)

Table 1 Heavy mineral composition (%) of Feixianguan sandstone in Huize area

样号	锆石	磷灰石	金红石	白钛石	辉石	电气石	铬尖晶石	赤—褐铁矿	磁铁矿	其他
10HLS2	0.01	0.01	0.01	—	—	—	0.07	98.46	1.34	0.11
10HLS16	0.94	0.02	—	0.01	4.38	—	0.02	75.70	1.38	17.55

注:“—”代表重矿物含量较少,仅能以颗粒数计算,低于检测限。

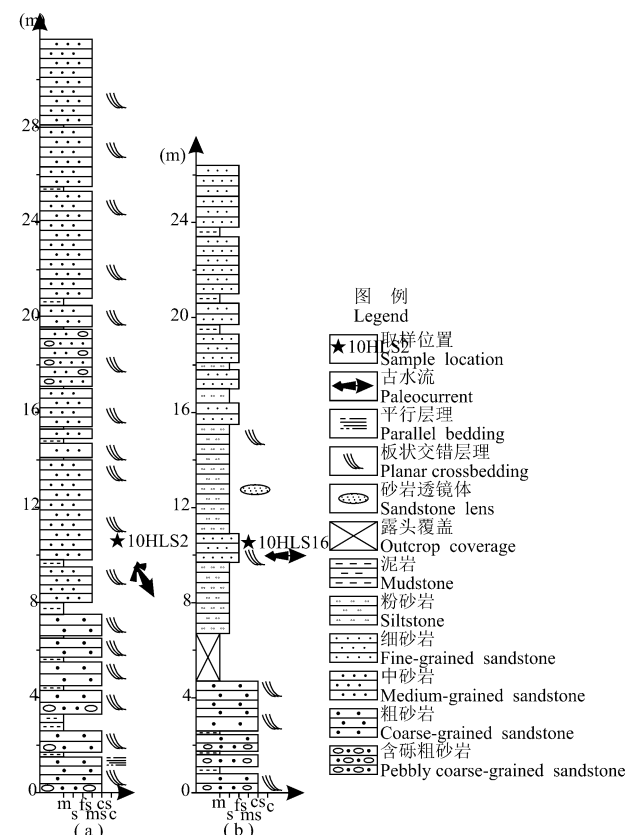


图3 会泽地区飞仙关组沉积序列图
(剖面位置见图1,采样位置见图中)

Fig. 3 Measured stratigraphic sections of the Feixianguan Formation in Huize area (Location of sections are indicated in Fig. 1)

m—泥岩;s—粉砂岩;fs—细砂岩;ms—中砂岩;
cs—粗砂岩;c—砾岩

Sample numbers for heavy mineral analysis and detrital zircon dating are well represented on the measured section. m—mudstone, s—siltstone, fs—fine—grained sandstone, ms—medium—grained sandstone, cs—coarse—grained sandstone

4 铬尖晶石电子探针

4.1 测试方法

电子探针测试在中国地质大学(北京)电子探针实验室完成,仪器型号为日本岛津公司生产的EPMA-1600。测试条件为加速电压15kV,激发电流

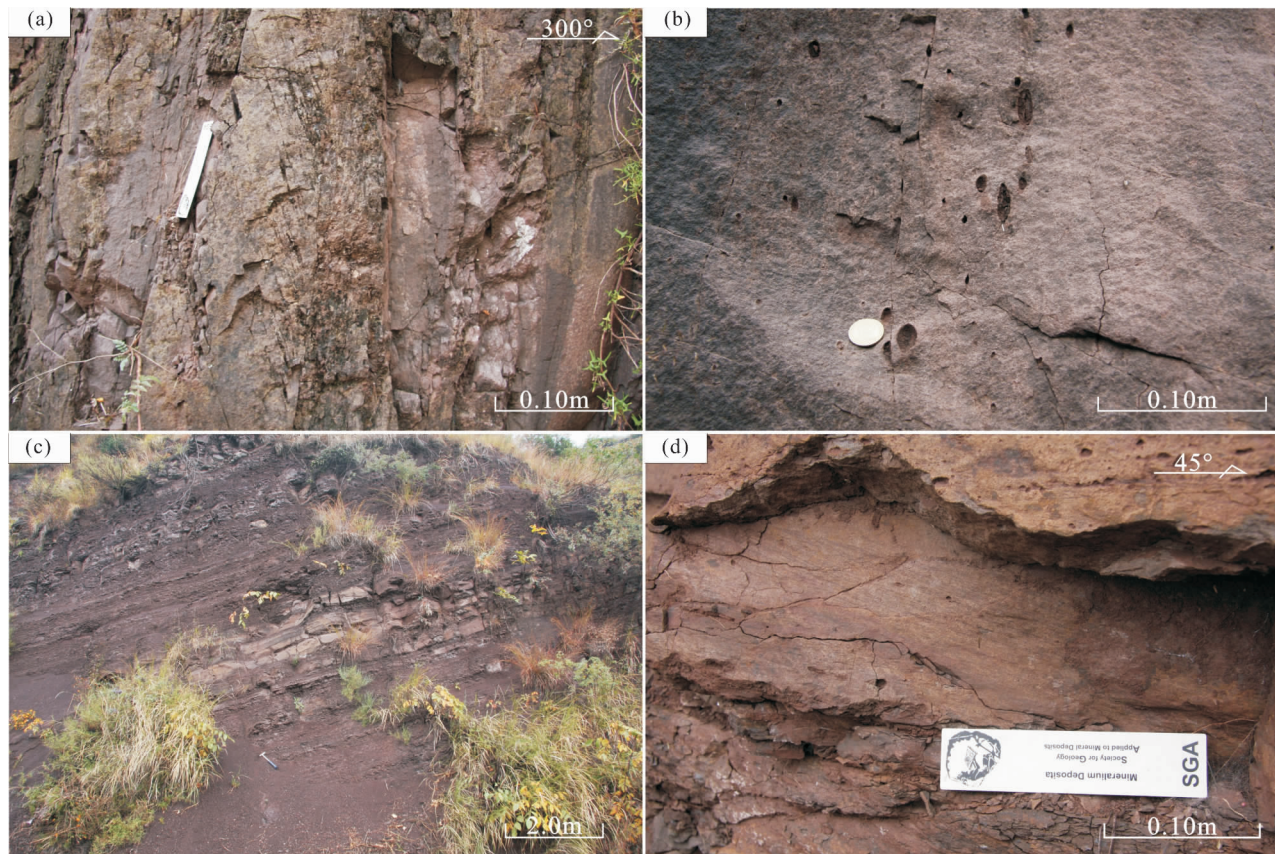


图 4 会泽地区飞仙关组野外典型照片

Fig. 4 Field photographs of various facies within the Feixianguan Formation

- (a) 粗砂岩,发育板状交错层理;(b) 中砂岩,含有泥砾;(c) 粉砂岩发育细砂岩透镜体;(d) 细砂岩,发育板状交错层理
 (a) Coarse-grained sandstone with planar cross bedding; (b) medium-grained sandstone with mudstone conglomerate; (c) siltstone with fine-grained sandstone lens; (d) planar cross bedding in fine-grained sandstone

10nA, 电子束直径 $1\mu\text{m}$, ZAF 法修正。分析标样采用磁铁矿(Fe)、钠长石(Si、Na、Al)、磷灰石(Ca、P)、金红石(Ti)、蔷薇辉石(Mn)、透长石(K)、橄榄石(Mg)、萤石(F)、独居石(La、Ce、Pr、Nd、Th)、锆石(Y、Zr、Hf)、铯榴石(Rb、Cs)、单矿物(U、Ta、Nb)等。主元素(质量分数 $> 20\%$)的允许的相对误差 $\leq 5\%$, 质量分数在 $3\% \sim 20\%$ 之间的元素允许的相对误差 $\leq 10\%$, 质量分数在 $1\% \sim 3\%$ 的元素允许的相对误差 $\leq 30\%$, 而质量分数在 $0.5\% \sim 1\%$ 之间的元素允许的相对误差 $< 50\%$ 。

4.2 测试结果

显微镜下, 铬尖晶石为黑褐色不透明矿物, 颗粒呈棱角状至圆状(图 5)。铬尖晶石的背散射图片显示, 尖晶石没有明显的核—边结构(图 5), 且尖晶石内部和边部数据变化不大(如探针点 11 和 12)(表 2), 表明尖晶石很少受到后期变质和蚀变的改造。铬尖晶石颗粒表现出化学成分的差异性, 主要体现

在参数 $\text{Mg}^\# \{ \text{Mg}^\# = n(\text{Mg}) / [n(\text{Mg}) + n(\text{Fe}^{2+})] \}$ 、 $\text{Cr}^\# \{ \text{Cr}^\# = n(\text{Cr}) / [n(\text{Cr}) + n(\text{Al})] \}$ 、 TiO_2 等。探针数据结果显示, $\text{Mg}^\#$ 变化较大, 介于 $0.31 \sim 0.66$ 。 $\text{Cr}^\#$ 较高, 变化范围为 $0.62 \sim 0.82$, 均值为 0.71 , 说明地幔源区的部分熔融程度较高。 TiO_2 含量分布范围较大, 区间为 $0.67\% \sim 3.82\%$, 平均 2.05% 。

探针数据结果表明, $\text{Mg}^\#$ 与 MnO 、 NiO 、 ZnO 和 V_2O_3 表现出不同的相关性(图 6)。 $\text{Mg}^\#$ 与 MnO 负相关(相关系数为 -0.62), 说明受后期改造较少。除探针点 11 外, NiO 含量为 $0.18\% \sim 0.61\%$, 与 $\text{Mg}^\#$ 正相关(相关系数为 0.30), 这可能与铬尖晶石结构中较大八面体的择优占位有关(Paktunc and Cabri, 1995)。除颗粒 5 和 10 外, ZnO 含量为 $0.03 \sim 2.68$, ZnO 与 $\text{Mg}^\#$ 为负相关, 表明锌具有较强的四面体择优占位(Paktunc and Cabri, 1995)。钒与 $\text{Mg}^\#$ 为正相关。总之, Mn 、 Zn 与 $\text{Mg}^\#$ 呈负相关, V 、 Ni 与 $\text{Mg}^\#$ 为正相关, 这与其不同的择优占位有关。同时

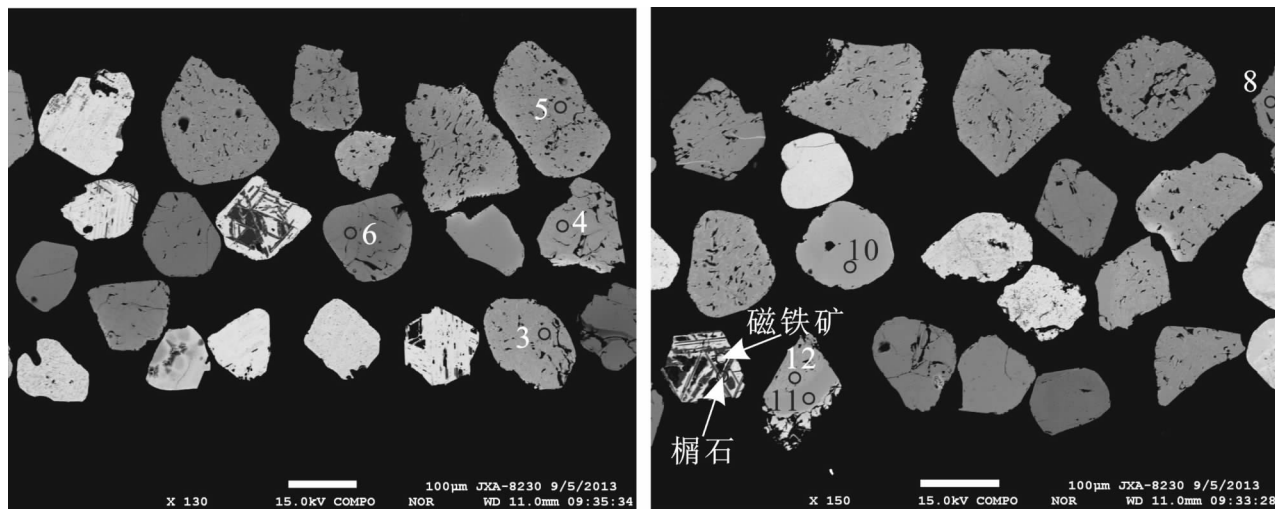


图 5 会泽地区飞仙关组铬尖晶石 BSE 图像(圆圈为打点位置,数字为点号)

Fig. 5 Backscattered electron (BSE) images of detrital chromian spinels from the Feixianguan Formation sandstone (circle for location, number for spot)

也表明,飞仙关组的物源区可能不唯一。

基于 TiO_2 和 Fe^{2+}/Fe^{3+} 的划分标准 (Lenaz et al., 2000), 飞仙关组尖晶石 $TiO_2 > 0.2\%$, $Fe^{2+}/Fe^{3+} > 4$, 因此, 尖晶石主要为火山成因。

由于尖晶石 TiO_2 的含量在玻安岩、岛弧玄武岩 → 板内玄武岩、洋中脊玄武岩和弧后盆地玄武岩逐渐增加, 因此可以利用 Cr、Al 和 Ti 的相互关系确定岩浆亲源性 (Arai, 1992)。在 TiO_2 与 $Cr/(Cr + Al)$ 图解 (图 7a), 大多数尖晶石数据位于板内玄武岩, 少数位于岛弧玄武岩。 Fe^{3+} —Cr—Al 图解则显示, 大部分尖晶石落于洋岛玄武岩 (OIB) 和岛弧玄武岩 (IAB) 的重叠区域 (图 7b)。基于 TiO_2 和 Al_2O_3 的图解, 大部分尖晶石数据投影于洋岛玄武岩 (OIB), 少量位于岛弧环境 (Arc), 个别为大火成岩省玄武岩 (LIP) (图 7b), 这与铬尖晶石 $Cr^{\#} > 0.6$ 指示源岩为层状侵入杂岩、大洋高原玄武岩以及与岛弧有关岩石一致 (Lee, 1999)。

因此, 铬尖晶石探针分析表明, 会泽地区飞仙关组的物源区主要为与洋岛/板内、次要为岛弧相关火山岩。

5 碎屑锆石

5.1 测试方法

样品碎样和锆石挑选工作由河北省区域地质矿产调查研究所实验室完成。锆石样品的制靶工作由中国地质科学院地质研究所大陆动力学实验室完

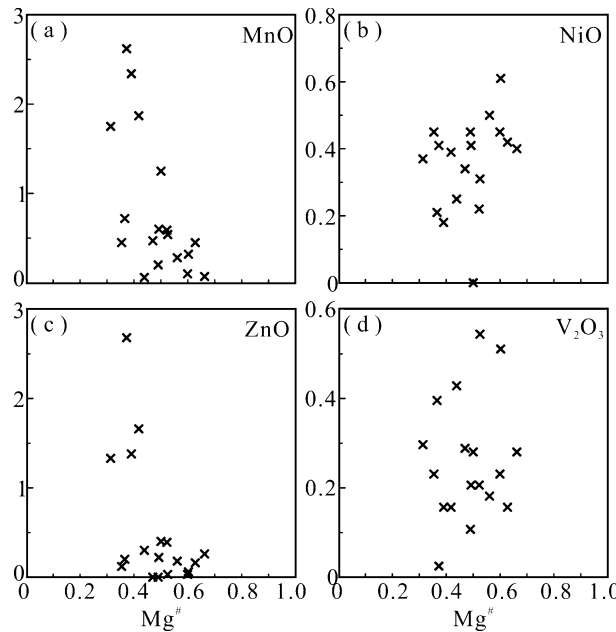


图 6 会泽地区飞仙关组铬尖晶石 $Mg^{\#}$ 与 MnO 、 NiO 、 ZnO 和 V_2O_3 协变图

Fig. 6 Chromian spinels covariant diagrams of $Mg^{\#}$ vs. MnO , NiO , ZnO , and V_2O_3 in Feixianguan sandstone of Huize area

成。锆石的阴极发光图像在中国地质科学院地质研究所的 HITACHI S3000-N 型扫描电子显微镜并配有 GATAN 公司 Chroma 阴极发光探头分析仪器上完成。锆石的 U-Pb 年龄测定时, 依据透射光图像、

反射光图像和阴极发光图像分析,对碎屑锆石样品随机圈定裂隙和包裹体不发育的颗粒。LA-MC-ICP-MS 锆石 U-Pb 定年测试分析在中国地质科学院矿产资源研究所成矿作用重点实验室完成,详细实验测试过程同侯可军等(2009)。采用 GJ-1 作为外部锆石年龄标准进行 U/Pb 同位素分馏校正(Jackson et al., 2004)。利用 NIST612 玻璃标样作为外标计算锆石样品的 Pb、U、Th 含量。数据处理采用 ICPMSDataCal 程序(Liu Yongsheng et al., 2009),普通 Pb 校正采用 Anderson 方法(Anderson, 2002),锆石年龄谐和图由 Isoplot 3.0 程序完成(Ludwig, 2003)。

对于锆石年龄 $> 1000\text{Ma}$ 的数据,采用 $^{207}\text{Pb}/^{206}\text{Pb}$ 年龄,而对于 $< 1000\text{Ma}$ 的数据,采用 $^{206}\text{Pb}/^{238}\text{U}$ 年龄(Gehrels et al., 1999; Sircombe, 1999)。以 $^{206}\text{Pb}/^{238}\text{U}$ 年龄和 $^{207}\text{Pb}/^{206}\text{Pb}$ 年龄比值为标准遴选 U-Pb 年龄

数据(Gehrels et al., 1999; Nelson et al., 2007; Kalsbeek et al., 2008; González-Len et al., 2009; Naipauer et al., 2010),不谐和度绝对值 $\leq 10\%$ 的数据为有效数据。表 3 列出了全部测试数据。字体加粗数据为不谐和数据,谐和图和直方图绘制以及探讨源区和区域的构造事件时均不予考虑。

5.2 测试结果及分析

对砂岩样品 10HLS2 进行 LA-ICP-MS U-Pb 分析,共测试 99 个颗粒,获得有效数据 88 个。年龄主要分布在 $248 \pm 4\text{Ma} \sim 2857 \pm 20\text{Ma}$ (图 8),其中表现出 $248 \sim 272\text{Ma}$ 和 $715 \sim 997\text{Ma}$ 两个明显的主峰值年龄段,以及 $512 \sim 542\text{Ma}$ 、 $548 \sim 650\text{Ma}$ 和 $1793 \sim 2481\text{Ma}$ 的次峰值年龄,少数锆石年龄为 $1039 \sim 1071\text{Ma}$ 和 $2507 \sim 2857\text{Ma}$ (图 8b, c, d)。根据区域演化历史, $248 \sim 272\text{Ma}$ 这组年龄记录了晚二叠世峨眉山玄武岩以及同期岩浆作用的过程(Fan Weiming

表 2 会泽地区飞仙关组砂岩 10HLS2 铬尖晶石电子探针数据表

Table 2 Chromian spinel electron probe data of Feixianguan sandstone 10HLS2 in Huize area

	02-1	02-2	02-3	02-4	02-5	02-6	02-7	02-8	02-9	02-10	02-11	02-12	02-13	02-14	02-15	02-16	02-17	02-18
SiO ₂	0.23	0.17	0.47	0.27	0.11	0.09	0.13	0.18	0.13	0.14	0.12	0.11	0.06	0	0.25	0.09	0.1	0.26
TiO ₂	2.18	0.79	1.68	1.47	2.09	0.75	3.32	2.04	1.85	4.26	2.45	2.22	3.05	0.67	3.82	0.67	2.51	1.13
Al ₂ O ₃	10.05	17.16	7.09	9.75	14.08	17.96	11.61	11.93	11.86	8.61	9.92	8.31	13.11	18.91	11.42	13.18	8.03	16.75
Cr ₂ O ₃	44.48	45.56	49.11	48.55	43.24	46.14	36.27	48.68	47.22	36.27	36.81	42.38	36.9	46.13	32.27	49.81	49.51	45.87
V ₂ O ₃	0.23	0.43	0.02	0.30	0.29	0.28	0.40	0.23	0.16	0.11	0.28	0.16	0.54	0.21	0.18	0.21	0.16	0.51
FeO	33.2	24.95	28.89	29.32	29.09	19.05	37.95	22.55	25.3	38.61	36.95	34.55	33.01	21.62	37.19	24.03	24.76	21.3
MnO	0.45	0.06	2.62	1.75	0.47	0.07	0.72	0.1	1.87	0.2	1.25	2.34	0.54	0.59	0.28	0.6	0.45	0.32
MgO	7.25	9.14	6.59	5.83	10.06	14.27	7.73	12.96	7.86	10.93	10.31	7.32	11.45	10.9	12.5	9.95	13.38	12.98
NiO	0.45	0.25	0.41	0.37	0.34	0.4	0.21	0.45	0.39	0.45	0	0.18	0.31	0.22	0.5	0.41	0.42	0.61
ZnO	0.12	0.3	2.68	1.33	0	0.26	0.2	0.03	1.66	0	0.4	1.38	0.03	0.39	0.18	0.22	0.16	0.06
CaO	0.04	0	0	0.06	0	0.08	0.07	0.05	0.02	0	0.15	0.1	0.09	0.01	0.07	0	0.14	0.01
Sum	98.68	98.81	99.56	99	99.77	99.35	98.61	99.2	98.32	99.58	98.64	99.05	99.09	99.65	98.66	99.17	99.62	99.8
FeO	23.55	20.85	19.77	22.76	20.22	12.98	23.86	15.45	19.51	20.30	18.34	20.37	18.45	17.77	17.44	18.29	14.16	15.28
Fe ₂ O ₃	10.73	4.55	10.14	7.29	9.86	6.75	15.65	7.89	6.43	20.35	20.69	15.76	16.18	4.28	21.95	6.38	11.78	6.69
Sum	99.76	99.26	100.58	99.73	100.76	100.03	100.17	99.99	98.96	101.62	100.72	100.63	100.71	100.08	100.86	99.81	100.8	100.47
Si	0.01	0.01	0.02	0.0	0.00	0.00	0.00	0.01	0.00	0.00	0.00	0.00	0.00	0.01	0.00	0.00	0.01	0.01
Ti	0.06	0.02	0.04	0.04	0.05	0.02	0.08	0.05	0.05	0.11	0.06	0.06	0.07	0.02	0.09	0.02	0.06	0.03
Al	0.40	0.66	0.29	0.39	0.54	0.66	0.46	0.45	0.47	0.33	0.39	0.33	0.50	0.71	0.43	0.51	0.31	0.62
Cr	1.19	1.17	1.33	1.32	1.11	1.14	0.96	1.24	1.26	0.94	0.96	1.14	0.94	1.15	0.82	1.29	1.27	1.14
Fe ³⁺	0.27	0.11	0.26	0.19	0.24	0.16	0.39	0.19	0.16	0.50	0.51	0.40	0.39	0.10	0.53	0.16	0.29	0.16
Fe ²⁺	0.67	0.57	0.57	0.65	0.55	0.34	0.67	0.42	0.55	0.56	0.51	0.58	0.50	0.47	0.47	0.50	0.38	0.40
Mn	0.01	0.00	0.08	0.05	0.01	0.00	0.02	0.00	0.05	0.01	0.03	0.07	0.01	0.02	0.01	0.02	0.01	0.01
Mg	0.37	0.44	0.34	0.30	0.49	0.66	0.39	0.62	0.40	0.54	0.51	0.37	0.55	0.51	0.60	0.49	0.65	0.61
V	0.01	0.01	0.00	0.01	0.01	0.01	0.01	0.01	0.00	0.00	0.01	0.00	0.01	0.01	0.00	0.01	0.00	0.01
Ni	0.01	0.01	0.01	0.01	0.01	0.01	0.01	0.01	0.01	0.01	0.00	0.00	0.01	0.01	0.01	0.01	0.01	0.02
Zn	0.00	0.01	0.07	0.03	0.00	0.01	0.00	0.00	0.04	0.00	0.01	0.03	0.00	0.01	0.00	0.01	0.00	0.00
Ca	0.00	0.00	0.00	0.00	0.00	0.00	0.00	0.00	0.00	0.00	0.01	0.00	0.00	0.00	0.00	0.00	0.00	0.00
Sum	3.00	3.00	3.00	3.00	3.00	3.00	3.00	3.00	3.00	3.00	3.00	3.00	3.00	3.00	3.00	3.00	3.00	3.00
Mg [#]	0.35	0.44	0.37	0.31	0.47	0.66	0.37	0.60	0.42	0.49	0.50	0.39	0.53	0.52	0.56	0.49	0.63	0.60
Cr [#]	0.75	0.64	0.82	0.77	0.67	0.63	0.68	0.73	0.73	0.74	0.71	0.77	0.65	0.62	0.65	0.72	0.80	0.65

注:Fe₂O₃ 根据尖晶石的化学计量比计算。

表 3 会泽地区飞仙关组砂岩碎屑锆石 LA-ICP-MS U-Pb 数据表

Table 3 Detrital zircon U-Pb isotopic data from the Feixianguan Formation in Huize area

测点编号	元素含量($\times 10^{-6}$)			Th/U	同位素比值						同位素年龄(Ma)						谐和度 (%)		
	Pb	Th	U		$n(^{207}\text{Pb})/n(^{206}\text{Pb})$		$n(^{207}\text{Pb})/n(^{235}\text{U})$		$(^{206}\text{Pb})/n(^{238}\text{U})$		$n(^{207}\text{Pb})/n(^{206}\text{Pb})$		$n(^{207}\text{Pb})/n(^{235}\text{U})$		$(^{206}\text{Pb})/n(^{238}\text{U})$				
					测值	1 σ	测值	1 σ	测值	1 σ	测值	1 σ	测值	1 σ	测值	1 σ			
10HLS2-1	36	110	346	0.32	0.0611	0.0013	0.8620	0.0292	0.1023	0.0017	642	41	631	16	628	10	100		
10HLS2-2	8	40	52	0.77	0.0704	0.0038	1.3636	0.0960	0.1414	0.0028	940	104	873	41	853	16	102		
10HLS2-3	25	142	158	0.90	0.0689	0.0022	1.2803	0.0565	0.1348	0.0019	894	63	837	25	815	11	103		
10HLS2-4	26	82	253	0.32	0.0598	0.0015	0.8399	0.0316	0.1018	0.0015	596	51	619	17	625	9	99		
10HLS2-5	83	195	848	0.23	0.0605	0.0010	0.8246	0.0224	0.0988	0.0012	620	35	611	12	608	7	100		
10HLS2-6	11	38	104	0.36	0.0621	0.0029	0.8907	0.0559	0.1061	0.0019	678	96	647	30	650	11	100		
10HLS2-7	17	241	377	0.64	0.0525	0.0018	0.2944	0.0145	0.0408	0.0007	305	75	262	11	257	4	102		
10HLS2-8	28	106	186	0.57	0.0679	0.0020	1.2942	0.0540	0.1383	0.0020	866	58	843	24	835	11	101		
10HLS2-9	16	196	128	1.52	0.0591	0.0026	0.7232	0.0442	0.0892	0.0017	570	92	553	26	551	10	100		
10HLS2-10	7	217	123	1.77	0.0578	0.0041	0.3239	0.0296	0.0415	0.0010	523	149	285	23	262	6	109		
10HLS2-11	67	256	355	0.72	0.0739	0.0015	1.7532	0.0549	0.1713	0.0023	1039	38	1028	20	1019	13	102		
10HLS2-12	14	84	90	0.94	0.0638	0.0024	1.1957	0.0635	0.1367	0.0026	735	74	799	29	826	15	97		
10HLS2-13	10	50	54	0.93	0.0735	0.0027	1.6777	0.0924	0.1674	0.0037	1029	69	1000	35	997	21	100		
10HLS2-14	8	34	80	0.43	0.0608	0.0026	0.7808	0.0498	0.0949	0.0024	632	87	586	28	584	14	100		
10HLS2-15	16	239	364	0.66	0.0579	0.0019	0.3314	0.0160	0.0419	0.0008	524	67	291	12	264	5	110		
10HLS2-16	11	54	130	0.42	0.0588	0.0022	0.7237	0.0385	0.0887	0.0017	561	77	553	23	548	10	101		
10HLS2-17	19	46	165	0.28	0.0638	0.0016	1.0236	0.0394	0.1173	0.0019	734	49	716	20	715	11	100		
10HLS2-18	14	38	134	0.28	0.0690	0.0023	1.0102	0.0495	0.1059	0.0019	899	66	709	25	649	11	109		
10HLS2-19	12	46	93	0.49	0.0646	0.0025	1.1171	0.0615	0.1264	0.0024	760	78	762	29	767	14	99		
10HLS2-20	39	912	809	1.13	0.0512	0.0012	0.2864	0.0105	0.0406	0.0006	251	52	256	8	256	4	100		
10HLS2-21	16	34	46	0.74	0.1167	0.0033	5.0351	0.2304	0.3145	0.0068	1906	47	1825	39	1763	33	108		
10HLS2-22	2	40	45	0.89	0.1165	0.0070	0.6404	0.0611	0.0425	0.0018	1903	103	503	38	268	11	188		
10HLS2-23	14	84	91	0.92	0.0612	0.0022	1.1567	0.0580	0.1380	0.0023	646	72	780	27	833	13	94		
10HLS2-24	3	19	16	1.20	0.1204	0.0077	1.8744	0.1856	0.1160	0.0049	1962	108	1072	66	707	28	278		
10HLS2-25	37	96	189	0.51	0.0671	0.0016	1.7378	0.0636	0.1878	0.0028	841	47	1023	24	1109	15	76		
10HLS2-26	21	134	142	0.94	0.0644	0.0016	1.1194	0.0445	0.1264	0.0022	755	50	763	21	767	13	99		
10HLS2-27	18	72	180	0.40	0.0611	0.0018	0.8607	0.0373	0.1024	0.0018	642	59	630	20	629	10	100		
10HLS2-28	21	124	144	0.86	0.0660	0.0020	1.1667	0.0531	0.1291	0.0024	805	59	785	25	783	14	100		
10HLS2-29	42	138	399	0.35	0.0574	0.0013	0.8411	0.0295	0.1061	0.0016	505	47	620	16	650	9	95		
10HLS2-30	7	205	131	1.56	0.0592	0.0032	0.3225	0.0236	0.0411	0.0009	576	111	284	18	260	6	109		
10HLS2-31	2	35	36	0.98	0.1502	0.0089	0.8568	0.0811	0.0450	0.0019	2348	96	628	44	284	12	221		
10HLS2-32	6	23	35	0.65	0.0725	0.0034	1.3892	0.0923	0.1431	0.0033	999	90	884	39	862	19	103		

测点编号	元素含量($\times 10^{-6}$)			Th/U	同位素比值						同位素年龄(Ma)							
	Pb	Th	U		$n(^{207}\text{Pb})/n(^{206}\text{Pb})$		$n(^{207}\text{Pb})/n(^{235}\text{U})$		$(^{206}\text{Pb})/n(^{238}\text{U})$		$n(^{207}\text{Pb})/n(^{206}\text{Pb})$		$n(^{207}\text{Pb})/n(^{235}\text{U})$		$(^{206}\text{Pb})/n(^{238}\text{U})$		谐和度 (%)	
					测值	1σ	测值	1σ	测值	1σ	测值	1σ	测值	1σ	测值	1σ		
10HLS2-33	23	218	121	1.81	0.0650	0.0022	1.2108	0.0615	0.1339	0.0027	773	67	806	28	810	15	100	
10HLS2-34	4	13	25	0.50	0.0882	0.0052	1.6803	0.1450	0.1398	0.0046	1387	107	1001	55	843	26	165	
10HLS2-35	54	123	91	1.36	0.1533	0.0020	9.2914	0.2469	0.4385	0.0078	2383	21	2367	24	2344	35	102	
10HLS2-36	14	63	99	0.63	0.0640	0.0022	1.0913	0.0545	0.1247	0.0023	740	69	749	26	757	13	99	
10HLS2-37	60	92	111	0.83	0.1540	0.0018	9.2943	0.2334	0.4418	0.0084	2390	18	2367	23	2358	38	101	
10HLS2-38	10	48	63	0.76	0.0642	0.0027	1.1917	0.0715	0.1351	0.0029	749	84	797	33	817	16	98	
10HLS2-39	26	155	265	0.59	0.0574	0.0020	0.6847	0.0333	0.0871	0.0014	507	73	530	20	538	8	99	
10HLS2-40	39	606	844	0.72	0.0525	0.0013	0.2769	0.0111	0.0393	0.0007	307	54	248	9	248	4	100	
10HLS2-41	37	206	383	0.54	0.0597	0.0015	0.7035	0.0267	0.0860	0.0013	594	52	541	16	532	8	102	
10HLS2-42	36	20	54	0.38	0.2038	0.0026	15.9241	0.4082	0.5706	0.0095	2857	20	2872	24	2910	39	98	
10HLS2-43	25	115	156	0.74	0.0720	0.0023	1.3469	0.0582	0.1355	0.0017	987	62	866	25	819	10	106	
10HLS2-44	29	288	284	1.01	0.0583	0.0027	0.6695	0.0409	0.0834	0.0015	540	96	520	25	516	9	101	
10HLS2-45	7	27	47	0.57	0.0711	0.0033	1.2437	0.0792	0.1309	0.0025	959	91	821	36	793	14	104	
10HLS2-46	91	131	152	0.86	0.1658	0.0022	10.7761	0.2327	0.4693	0.0049	2516	21	2504	20	2481	22	101	
10HLS2-47	85	110	145	0.76	0.1650	0.0023	10.6982	0.2622	0.4681	0.0061	2507	22	2497	23	2475	27	101	
10HLS2-48	8	51	55	0.92	0.0657	0.0032	1.1070	0.0729	0.1237	0.0025	797	97	757	35	752	14	101	
10HLS2-49	19	57	88	0.66	0.0751	0.0024	1.9374	0.0854	0.1873	0.0027	1071	60	1094	30	1107	15	97	
10HLS2-50	16	135	95	1.42	0.0668	0.0028	1.1468	0.0658	0.1256	0.0022	831	84	776	31	763	12	102	
10HLS2-51	155	322	245	1.31	0.1598	0.0024	10.1590	0.2403	0.4579	0.0048	2453	24	2449	22	2430	21	101	
10HLS2-52	15	54	86	0.62	0.0685	0.0031	1.4253	0.0866	0.1506	0.0028	883	88	900	36	904	16	100	
10HLS2-53	16	169	86	1.96	0.0686	0.0034	1.1716	0.0729	0.1242	0.0018	888	97	787	34	755	11	104	
10HLS2-54	6	192	107	1.80	0.0701	0.0031	0.3840	0.0236	0.0408	0.0008	930	86	330	17	258	5	128	
10HLS2-55	25	132	171	0.77	0.0641	0.0017	1.1021	0.0436	0.1253	0.0021	743	53	754	21	761	12	99	
10HLS2-56	22	102	154	0.66	0.0648	0.0021	1.1109	0.0499	0.1237	0.0018	769	66	759	24	752	10	101	
10HLS2-57	14	98	91	1.08	0.0622	0.0028	1.0540	0.0600	0.1212	0.0018	681	92	731	30	738	10	99	
10HLS2-58	26	128	183	0.70	0.0650	0.0018	1.0916	0.0455	0.1222	0.0020	775	57	749	22	743	11	101	
10HLS2-59	190	194	346	0.56	0.1608	0.0023	10.3300	0.2355	0.4611	0.0049	2464	23	2465	21	2444	22	101	
10HLS2-60	11	359	181	1.98	0.0539	0.0030	0.3207	0.0238	0.0431	0.0009	367	123	282	18	272	6	104	
10HLS2-61	19	101	197	0.51	0.0586	0.0016	0.6952	0.0334	0.0869	0.0023	551	56	536	20	537	14	100	
10HLS2-62	24	225	111	2.04	0.2365	0.0157	5.8732	0.5751	0.1630	0.0061	3097	103	1957	85	973	34	318	
10HLS2-63	6	115	127	0.90	0.0600	0.0029	0.3270	0.0221	0.0406	0.0010	605	100	287	17	257	6	112	
10HLS2-64	38	222	254	0.87	0.0647	0.0013	1.1293	0.0362	0.1256	0.0017	765	42	767	17	762	10	101	
10HLS2-65	3	42	75	0.56	0.0865	0.0052	0.4871	0.0395	0.0413	0.0010	1350	114	403	27	261	6	154	
10HLS2-66	7	39	41	0.96	0.0909	0.0048	1.7044	0.1223	0.1358	0.0030	1443	98	1010	46	821	17	176	

测点编号	元素含量($\times 10^{-6}$)			Th/U	同位素比值						同位素年龄(Ma)							
	Pb	Th	U		$n(^{207}\text{Pb})/n(^{206}\text{Pb})$		$n(^{207}\text{Pb})/n(^{235}\text{U})$		$(^{206}\text{Pb})/n(^{238}\text{U})$		$n(^{207}\text{Pb})/n(^{206}\text{Pb})$		$n(^{207}\text{Pb})/n(^{235}\text{U})$		$(^{206}\text{Pb})/n(^{238}\text{U})$		谐和度 (%)	
					测值	1σ	测值	1σ	测值	1σ	测值	1σ	测值	1σ	测值	1σ		
10HLS2-67	13	54	93	0.58	0.0658	0.0027	1.1322	0.0627	0.1239	0.0020	800	84	769	30	753	12	102	
10HLS2-68	16	100	102	0.98	0.0653	0.0024	1.1753	0.0607	0.1302	0.0023	784	74	789	28	789	13	100	
10HLS2-69	24	139	161	0.86	0.0660	0.0021	1.1596	0.0540	0.1278	0.0023	805	64	782	25	775	13	101	
10HLS2-70	6	17	60	0.29	0.0614	0.0030	0.8234	0.0574	0.0980	0.0023	654	103	610	32	603	14	101	
10HLS2-71	35	250	215	1.17	0.0658	0.0022	1.1677	0.0525	0.1283	0.0018	798	68	786	25	778	10	101	
10HLS2-72	96	167	158	1.05	0.1625	0.0023	10.6339	0.2535	0.4715	0.0057	2481	23	2492	22	2490	25	100	
10HLS2-73	26	124	179	0.70	0.0630	0.0018	1.0953	0.0442	0.1268	0.0019	709	58	751	21	769	11	98	
10HLS2-74	30	232	153	1.52	0.0683	0.0019	1.4013	0.0556	0.1485	0.0021	877	55	889	24	892	12	100	
10HLS2-75	9	94	69	1.36	0.0638	0.0037	0.8179	0.0620	0.0964	0.0019	735	121	607	35	593	11	102	
10HLS2-76	14	51	100	0.51	0.0658	0.0028	1.1744	0.0674	0.1292	0.0023	799	86	789	31	783	13	101	
10HLS2-77	45	201	292	0.69	0.0650	0.0014	1.2490	0.0396	0.1393	0.0017	773	44	823	18	841	9	98	
10HLS2-78	8	38	83	0.46	0.0671	0.0033	0.8148	0.0541	0.0891	0.0018	840	100	605	30	550	11	110	
10HLS2-79	8	35	47	0.74	0.0780	0.0032	1.5238	0.0915	0.1426	0.0033	1146	79	940	37	859	18	109	
10HLS2-80	18	76	196	0.39	0.0618	0.0020	0.7486	0.0346	0.0877	0.0014	668	68	567	20	542	8	105	
10HLS2-81	41	174	282	0.62	0.0674	0.0022	1.2572	0.0585	0.1369	0.0022	851	66	827	26	827	13	100	
10HLS2-82	43	182	335	0.54	0.0652	0.0020	1.1317	0.0487	0.1255	0.0017	781	64	769	23	762	10	101	
10HLS2-83	223	246	443	0.56	0.1596	0.0020	10.1870	0.2341	0.4608	0.0060	2452	21	2452	21	2443	26	100	
10HLS2-84	58	150	103	1.45	0.1608	0.0030	9.6531	0.2970	0.4362	0.0066	2464	30	2402	28	2334	29	106	
10HLS2-85	240	599	1600	0.37	0.0673	0.0010	1.4320	0.0318	0.1535	0.0015	847	29	902	13	921	8	98	
10HLS2-86	70	341	441	0.77	0.0717	0.0017	1.4591	0.0521	0.1474	0.0022	978	46	914	22	887	12	103	
10HLS2-87	70	112	218	0.51	0.1096	0.0018	4.6688	0.1409	0.3111	0.0052	1793	30	1762	25	1746	26	103	
10HLS2-88	44	237	482	0.49	0.0787	0.0113	0.9583	0.1517	0.0899	0.0015	1164	289	682	79	555	9	123	
10HLS2-89	74	203	485	0.42	0.0717	0.0020	1.5206	0.0604	0.1551	0.0021	978	56	939	24	930	12	101	
10HLS2-90	32	223	225	0.99	0.0675	0.0027	1.1831	0.0644	0.1274	0.0022	853	81	793	30	773	12	103	
10HLS2-91	58	25	515	0.05	0.0656	0.0023	1.1481	0.0556	0.1275	0.0020	793	71	776	26	773	12	100	
10HLS2-92	55	135	126	1.07	0.1314	0.0034	6.7752	0.2829	0.3773	0.0073	2116	44	2082	37	2064	34	103	
10HLS2-93	74	245	410	0.60	0.0743	0.0022	1.7597	0.0790	0.1746	0.0032	1048	58	1031	29	1037	18	101	
10HLS2-95	692	684	1778	0.39	0.1327	0.0013	7.0611	0.1283	0.3852	0.0042	2133	16	2119	16	2100	20	102	
10HLS2-96	30	355	309	1.15	0.0595	0.0039	0.6613	0.0560	0.0827	0.0018	585	140	515	34	512	11	101	
10HLS2-97	47	353	436	0.81	0.0604	0.0028	0.8297	0.0545	0.1021	0.0023	619	98	613	30	627	13	98	
10HLS2-98	67	343	888	0.39	0.0603	0.0023	0.6600	0.0390	0.0837	0.0022	615	79	515	24	518	13	99	
10HLS2-99	40	517	1056	0.49	0.0571	0.0046	0.2900	0.0311	0.0392	0.0012	497	173	259	24	248	8	104	
10HLS2-100	55	261	403	0.65	0.0715	0.0037	1.2939	0.0893	0.1326	0.0026	972	104	843	40	802	15	105	

et al., 2004; Zhong Hong et al., 2007; Shellnutt et al., 2008; Xu Yigang et al., 2008), 715~997 Ma 记录了新元古代 Rodinia 超大陆裂解(Li et al., 2002; 崔晓庄等, 2012; 任光明等, 2013; 程佳孝等, 2014)或者板块俯冲作用过程(Zhou et al., 2007; Zhao Junhong et al., 2007)。岩浆成因的碎屑锆石年龄为 1793 ± 30 Ma, 与区域辉绿岩(Zhao Xinfu et al., 2010; 郭阳等, 2014)、花岗斑岩(王子正等, 2013)等年龄相当, 可能与 Columbia 超大陆裂解有关(Zhao Xinfu et al., 2010; 王子正等, 2013)。

6 物源综合分析

主峰值 $248 \sim 272$ Ma 岩石占碎屑锆石显示总数 9%, 锆石颗粒 Th/U 比值介于 $0.49 \sim 1.78$, 锆石颗粒呈次棱角状一次圆状, 具有弱振荡环带(图 9), 为典型的岩浆成因, 加权峰值和概率峰值均为 257 ± 6 Ma(图 8c)。这与峨眉山 LIP 玄武岩及同期侵入岩形成时代 $242 \sim 260$ Ma(Fan Weiming et al., 2004; Zhong Hong et al., 2007; Shellnutt et al., 2008; Xu Yigang et al., 2008)相一致。峨眉山玄武岩中锆石含量较少且较小, 其风化剥蚀很难提供如此大颗粒的锆石, 这些锆石可能是玄武岩顶部凝灰岩提供(Xu Yigang et al., 2008; 朱江等, 2011)。依据研究区及邻区相关岩石的形成年龄和构造环境(表 4)可

以得知, 具有 LIP 特征的铬尖晶石主要来自峨眉山玄武岩及同时期基性岩, 虽然指示该物源区的铬尖晶石个数较少, 可能与分析的颗粒数较少有关。因此, 峨眉山大火成岩省玄武岩等基性岩或凝灰岩为飞仙关组沉积提供沉积物。

主年龄峰值 $715 \sim 997$ Ma 的碎屑锆石显示, 颗粒呈棱角状一次圆状, Th/U 比值介于 $0.28 \sim 1.96$, 部分锆石颗粒具有弱的振荡环带, 为典型的岩浆成因, 如锆石颗粒 36、73 和 2; 部分锆石颗粒具有扇形分带, 为变质成因, 如锆石颗粒 2(图 9)。而岩浆成因锆石颗粒的加权峰值为 758 ± 6 Ma、 811 ± 19 Ma、 893 ± 10 Ma(图 8d)。而且区域资料表明, 研究区西南东川下田坝花岗岩的 LA-ICP-MS U-Pb 年龄为 769 ± 4 Ma(程佳孝等, 2014) 或 762.1 ± 6.2 Ma、 801.1 ± 6.6 Ma(武昱东等, 2014); 研究区西北会东溜姑花岗岩的 LA-ICP-MS U-Pb 年龄为 806 ± 13 Ma(程佳孝等, 2014); 东川澄江组凝灰岩的 SHRIMP U-Pb 年龄为 803.1 ± 8.7 Ma(Jiang Xinsheng et al., 2012)。上述岩浆岩可能为飞仙关组提供大量物源。区域资料表明, 新元古代甘洛苏雄组玄武岩(年龄为 803 ± 12 Ma; Li et al., 2002)、冕宁辉绿岩(年龄为 774 ± 10 Ma; 任光明等, 2013)以及武定辉绿岩(年龄为 1767 ± 15 Ma; 郭阳等, 2014)地球化学分析结果表明, 岩石具有 OIB 型玄武质岩浆特征,

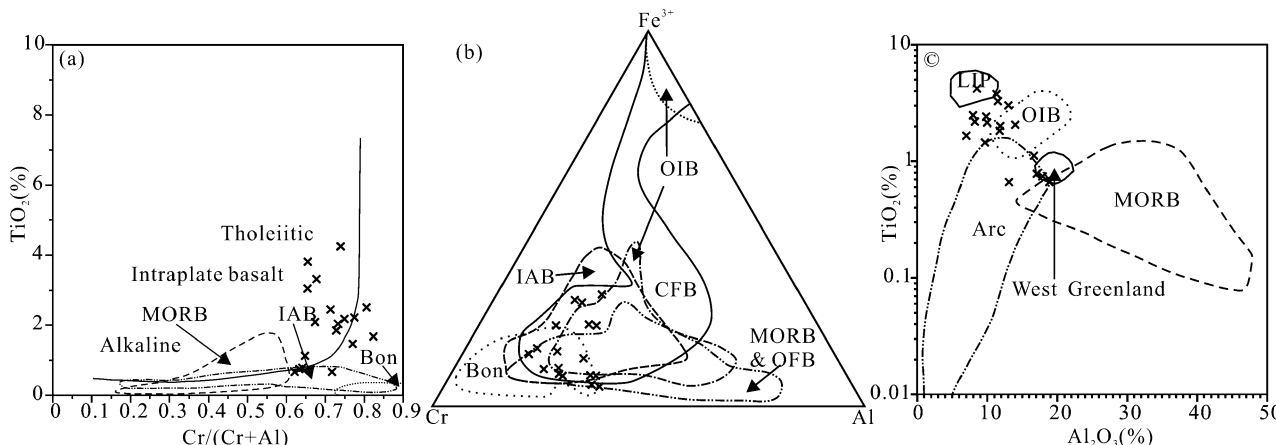


图 7 会泽地区飞仙关组铬尖晶石主量元素构造背景判别图解: (a) TiO_2 — $\text{Cr}/(\text{Cr} + \text{Al})$ 图解(Arai, 1992); (b) Fe^{3+} — Cr — Al 图解(Barnes et al., 2001); (c) TiO_2 — Al_2O_3 图解(据 Kamenetsky et al., 2001)

Fig. 7 Discrimination diagrams of detrital chromian spinels composition from the Feixianguan Formation in the Huize area: (a) TiO_2 — $\text{Cr}/(\text{Cr} + \text{Al})$ diagram, compositional fields are after Arai(1992); (b) Fe^{3+} — Cr — Al diagram for discriminating different type volcanic spinels; (c) TiO_2 — Al_2O_3 diagram, compositional fields are after Kamenetsky et al. (2001)

Tholeiitic—拉斑系列; Alkaline—碱性系列; Intraplate basalt—板内玄武岩; MORB—洋岛玄武岩; IAB—岛弧玄武岩; Bon—玻安岩; OIB—洋岛玄武岩; OFB—洋底玄武岩; CFB—大陆溢流玄武岩; LIP—大火成岩省; Arc—岛弧岩浆岩; West Greenland—西格陵兰岛; MORB—Mid-ocean ridge basalt; IAB—Island arc basalt; Bon—Boninite; OIB—Ocean island basalt; OFB—Ocean floor basalt; CFB—Continental flood basalt; LIP—Large igneous province; Arc—island arc magma

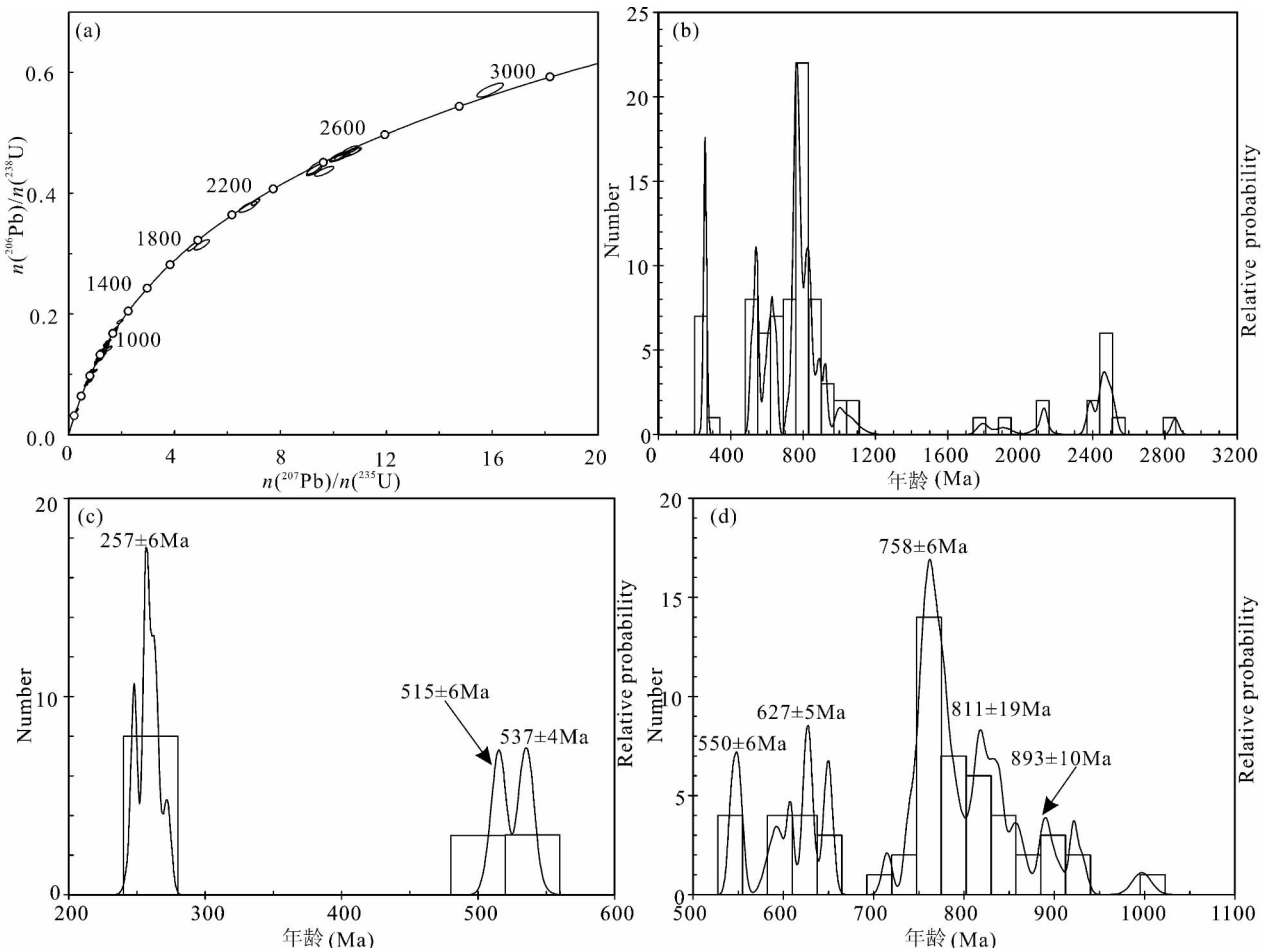


图 8 会泽地区飞仙关组样品 10HLS2 碎屑锆石 U-Pb 谱和曲线图以及 U-Pb 年龄谱图

Fig. 8 Concordia plots (a), histograms and relative probability plots (b, c, d) of detrital zircon U-Pb ages of the Early Triassic Feixianguan Formation sandstone sample (No. 10HLS2) in Huize area

与地幔柱幕式活动相关(表4)。林广春等(2006)确认780~760Ma基性岩墙群具有板内玄武岩(地球化学显示OIB)的特征,可能是高位地幔柱部分熔融的产物。因此,铬尖晶石指示与3类岩石同时期的基性岩浆岩为飞仙关组提供物源;结合碎屑锆石测年结果(前述)和古水流恢复的物源方向(图3),冕宁辉绿岩、苏雄组玄武岩等成为飞仙关组另一主要物源区。碎屑颗粒点2呈现出扇形分带,可能为变质成因,这与区域861±34Ma的变质年龄相一致(尹福光等,2011)。

次要峰值年龄512~542Ma的锆石颗粒Th/U比值介于0.39~1.15,锆石颗粒具有弱的振荡环带(图9),为岩浆成因。加权峰值分别为515±6Ma、537±4Ma(图8c),概率峰值分别为516Ma和536Ma。区域资料表明,遵义松林早寒武世牛蹄塘组底部凝灰岩年龄为518±5Ma(周明忠等,2008),

云南晋宁梅树村组底部少量钾质斑脱岩年龄为536.5±2.5Ma(Sawaki et al., 2008),贵州江平老堡组顶部钾质斑脱岩的年龄为536±5Ma(周明忠等,2013)。而且,江平老堡组顶部钾质斑脱岩的稀土元素配分曲线与晋宁梅树村组钾质斑脱岩相似(周明忠等,2013),区域上可以进行对比。因此,碎屑锆石指示早寒武世大规模火山岩浆作用在上扬子地区普遍存在。而研究区西部和西北部该时期沉积物可能因后期构造运动强烈风化严重或者其他原因,未能取得很好的年龄结果,但是成为飞仙关组的物源区之一。

源自548~650Ma的锆石颗粒呈棱角状一次圆状,Th/U比值介于0.23~1.56,部分锆石颗粒具有弱的振荡环带,为典型的岩浆成因,如锆石颗粒16和18(图9)。而岩浆成因锆石颗粒的加权峰值为

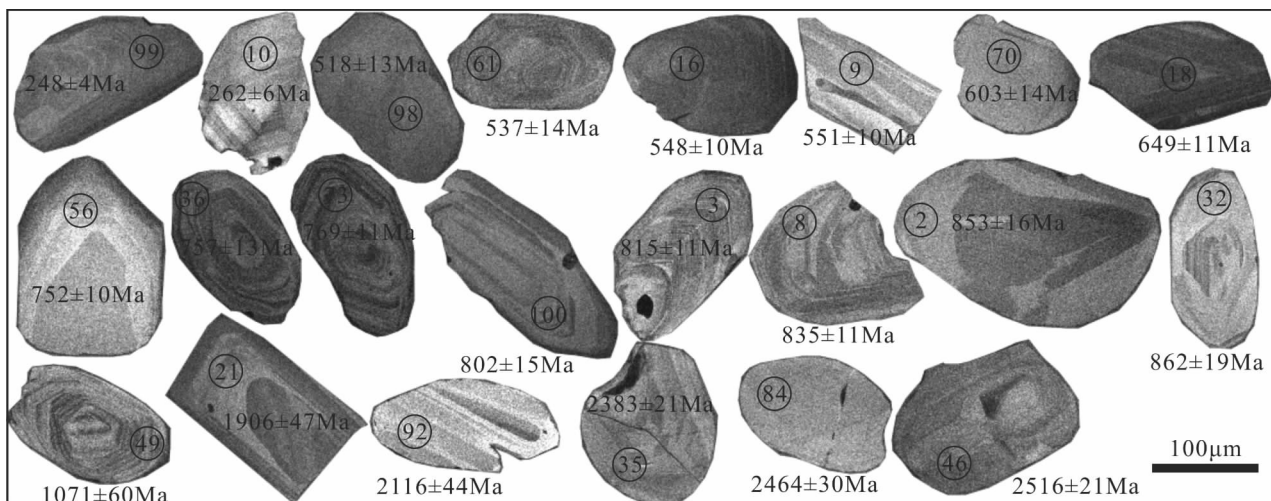


图 9 上扬子会泽地区飞仙关组碎屑锆石的 CL 图像

Fig. 9 Cathodoluminescence (CL) images of selected detrital zircons from the Early Triassic Feixianguan Formation in Huize area

表 4 扬子西缘基性岩和凝灰岩形成年龄和构造环境汇总表

Table 4 Ages and tectonic setting of basic rocks and tuff in the western Yangtze areas

样品岩性	所处位置/层位	年龄(Ma)	测试方法	构造环境	参考文献
玄武岩	桂西	253.6 ± 0.4 255.4 ± 0.4 256.2 ± 0.8	Ar-Ar	LIP(大火成岩省)	Fan Weiming et al., 2004
玄武岩	峨眉山			LIP	Xu et al., 2001
辉长岩	西昌沙坝	752 ± 11 752 ± 12	SHRIMP	Rodinia 裂解, 地幔柱幕式活动	Li et al., 2003
辉绿岩	冕宁叠相营群	774 ± 10	SHRIMP	板内拉张, Rodinia 裂解	任光明等, 2013
辉长岩	石棉大渡河	779 ± 6	SHRIMP	Rodinia 裂解, 地幔柱幕式活动	林广春等, 2006
苏雄组流纹岩、玄武岩	甘洛苏雄	803 ± 12	SHRIMP	Rodinia 裂解, 地幔柱幕式活动	Li et al., 2002
澄江组凝灰岩	滇中金阳	797.8 ± 8.2	SHRIMP	Rodinia 裂解	Jiang Xinsheng et al., 2012
澄江组凝灰岩	东川	803.1 ± 8.7	SHRIMP	Rodinia 裂解	
辉绿岩	峨边金口河	813.4 ± 8.2	SHRIMP	Rodinia 裂解	崔晓庄等, 2012
陆良组顶底凝灰岩	滇东陆良县	818.6 ± 9.2 805 ± 14	SHRIMP	半地堑大陆裂谷, Rodinia 裂解产物	卓皆文等, 2013
黑山头组凝灰岩	滇中昆阳群	1032 ± 9	SHRIMP	岛弧型	张传恒等, 2007
通安组三段 通安组五段	东川	1270 ± 95 1082 ± 13	SHRIMP	岛弧型	尹福光等 2011
黑山头组凝灰岩 天宝山组英安斑岩	滇中昆阳群 会理天宝山	1031 ± 12 1047 ± 15 1036 ± 12	SHRIMP	岛弧型	尹福光等 2012
黑山组凝灰岩	东川昆阳群	1503 ± 17	SHRIMP	初始裂谷	孙志明等, 2009
辉长岩	会理通安	1694 ± 16	LA-ICP-MS	Columbia 超大陆裂解伸展作用	王冬兵等, 2013
辉绿岩	武定(东川 西南 180km)	1767 ± 15	LA-ICP-MS	Columbia 超大陆裂解, 地幔柱活动	郭阳等, 2014

550 ± 6 Ma、 627 ± 5 Ma(图 8d)。前人研究成果表明,铜仁坝黄老堡组顶部凝灰岩的 SHRIMP U-Pb 年龄为 556 ± 5 Ma(卓皆文等,2009),贵州瓮安、福泉陡山沱组底部和顶部磷块岩的 Pb-Pb 年龄分别为 576 ± 14 Ma 和 601 ± 34 Ma(Chen Duofu et al., 2004)或者 551 ± 0.6 Ma 和 635 ± 1 Ma(Condon et al., 2005),但研究区及周缘同样没有年龄数据发表,可能与研究区新元古代晚期研究程度较弱有关,但指示该时期岩浆岩为物源区之一。

次要物源区 $1793 \sim 2431$ Ma 的锆石颗粒占总数的 12.580%,锆石年龄 1793 ± 30 Ma 的碎屑颗粒可能由河口群火山岩(锆石 LA-ICP-MS U-Pb 年龄为 1722 ± 25 Ma,王冬兵等,2012)提供物源。而会泽飞仙关组碎屑锆石 $1906 \sim 2481$ Ma 古元古代年龄值,迄今在扬子地块西缘还没有准确的相应岩浆岩记录,在研究区须家河组碎屑岩中,也发现了大量的 $1900 \sim 2500$ Ma 的碎屑锆石(未刊出资料)。这些锆石呈次圆状,可能经历了多次搬运过程。目前露头没有相应年龄发表,还不能准确确定物源区,但至少说明古元古代时期发育大量岩浆作用。

另外, $1039 \sim 1071$ Ma 的锆石颗粒仅有 3 个,Th/U 比值介于 0.60 ~ 0.72,锆石具有明显的振荡环带,为典型的岩浆锆石。尹福光等(2012b)认为 $1000 \sim 1100$ Ma 扬子西缘火山岩为岛弧性质。且铬尖晶石指示物源区之一为岛弧型基性岩类。据岩石构造环境汇总表可知,黑山头组、通安组和天宝山组岩石形成于岛弧环境(表 4)。其源区可能为黑头山组富良棚段火山岩(张传恒等,2007;尹福光等,2012b)、天宝山组火山岩(尹福光等,2012b)。

颗粒 42 的年龄为 2857 ± 20 Ma,这表明扬子西南缘可能存在古老的新太古代结晶基底,与扬子西缘峨边—金口河地区发现的两个单颗粒锆石 SHRIMP U-Pb 年龄(2737 ± 30 Ma 和 2480 ± 29 Ma)(熊国庆等,2013)大体相当。

7 结论

飞仙关组主要为紫红色中—粗砂岩与紫红色薄层泥岩,形成于辫状河环境,交错层理指示物源主要来自于西部和西北部。通过对会泽地区飞仙关组砂岩的重矿物综合分析,可以得出以下初步认识:

(1) 飞仙关组重矿物主要由赤—褐铁矿、磷灰石、白钛石、辉石、铬铁矿、磁铁矿组成,重矿物组合说明物源来自于岩浆岩;

(2) 铬尖晶石探针分析表明,Mg[#]与 MnO、NiO、

ZnO 和 V₂O₃ 呈现出不同的相关性,化学成分存在差异;铬尖晶石指示物源主要来自于与板内/洋岛相关玄武岩,次要为岛弧性质岩石;

(3) 砂岩碎屑锆石 LA-ICP-MS U-Pb 年龄和铬尖晶石指示,物源主要来自 $248 \sim 272$ Ma 大火成岩省峨眉山玄武岩及同期侵入岩,物源 $715 \sim 997$ Ma 岩石具有洋岛/板内性质岩浆岩,主要为研究区及周缘新元古代玄武岩、凝灰岩和辉绿岩等;

(4) 碎屑锆石 U-Pb 年龄测定表明,除了新元古代和晚二叠世发育岩浆作用之外,上扬子地区在古元古代和早寒武世也发育岩浆作用。

致谢:电子探针测试工作得到中国地质大学(北京)重点实验室郝金华老师的帮助!碎屑锆石测年工作得到中国地质科学院矿产资源研究所重点实验室侯可军博士的帮助!

注释 / Notes

① 云南省地质局区域地质调查队. 1981. 中华人民共和国 1:20 万地质图·东川幅.

参 考 文 献 / References

- (The literature whose publishing year followed by a “&” is in Chinese with English abstract; the literature whose publishing year followed by a “#” is in Chinese without English abstract)
- 陈洪德,张成弓,黄福喜,侯明才. 2011. 中上扬子克拉通海西—印支期(泥盆纪—中三叠世)沉积层序充填过程与演化模式. 岩石学报,27(8):2281~2298.
- 程佳孝,罗金海,武显东,韩奎,王师迪. 2014. 滇东北下田坝花岗岩年代学、地球化学及其构造意义. 地质学报,88(3):337~346.
- 辜学达,刘啸虎. 1997. 四川省岩石地层. 武汉:中国地质大学出版社.
- 何斌,徐义刚,肖龙,王康明,沙绍礼. 2003. 峨眉山大火成岩省的形成机制及空间分布:来自沉积地层学的新证据. 地质学报,77(2):194~202.
- 侯可军,李延河,田有荣. 2009. LA-MC-ICP-MS 锆石微区原位 U-Pb 定年技术. 矿床地质,28(4):481~492.
- 黄福喜,陈洪德,侯明才,钟怡江,李洁. 2011. 中上扬子克拉通加里东期(寒武—志留纪)沉积层序充填过程与演化模式. 岩石学报,27(8):2299~2317.
- 李文博,黄智龙,张冠. 2006. 云南会泽铅锌矿田成矿物质来源:Pb、S、C、H、O、Sr 同位素制约. 岩石学报,22(10):2567~2580.
- 李献华,周汉文,李正祥,刘颖. 2002. 川西新元古代双峰式火山岩成因的微量元素和 Sm-Nd 同位素制约及其大地构造意义. 地质科学,37(3):264~276.
- 林广春,李献华,李武显. 2006. 川西新元古代基性岩墙群的 SHRIMP 锆石 U-Pb 年龄、元素和 Nd-Hf 同位素地球化学:岩石成因与构造意义. 中国科学 D 辑:地球科学,36(7):630~645.
- 林良彪,陈洪德,姜平,胡晓强,纪相田,叶黎明. 2006. 川西前陆盆地须家河组沉积相及岩相古地理演化. 成都理工大学学报(自然科学版),33(4):376~383.
- 任光明,庞维华,孙志明,尹福光,肖启亮. 2013. 扬子西缘登相营群基性岩墙锆石 U-Pb 年代学及岩石地球化学特征. 成都理工大

- 学学报(自然科学版),40(1):66~79.
- 邵龙义,高彩霞,张超,汪浩,郭立君,高彩红. 2013. 西南地区晚二叠世层序——古地理及聚煤特征. 沉积学报,31(5):856~866.
- 时志强,伊海生,曾德勇,张华. 2010. 上扬子地区下三叠统飞仙关组一段:大灭绝后从停滞海洋到动荡海洋的沉积记录. 地质论评,56(6):769~780.
- 唐勇,覃建雄. 2007. 四川西昌盆地三叠系沉积环境分析. 四川地质学报,27(2):92~95.
- 田景春,陈洪德,彭军,覃建雄,侯中健,寿建峰,杨晓宁,沈安江,陈子焯. 2000. 川滇黔桂地区下、中三叠统层序划分、对比及层序地层格架. 沉积学报,18(2):198~204.
- 王冬兵,孙志明,尹福光,王立全,王保弟,张万平. 2012. 扬子地块西缘河口群的时代:来自火山岩锆石LA-ICP-MS U-Pb年龄的证据. 地层学杂志,36(3):630~635.
- 王冬兵,尹福光,孙志明,王立全,王保弟,廖世勇,唐渊,任光明. 2013. 扬子陆块西缘古元古代基性侵入岩LA-ICP-MS锆石U-Pb年龄和Hf同位素及其地质意义. 地质通报,32(4):617~630.
- 王剑,刘宝珺,潘桂棠. 2001. 华南新元古代裂谷盆地演化——Rodinia超大陆解体的前奏. 矿物岩石,21(3):135~145.
- 王子正,郭阳,杨斌,王生伟,孙晓明,侯林,周邦国,廖震文. 2013. 扬子克拉通西缘1.73Ga非造山型花岗斑岩的发现及其地质意义. 地质学报,87(7):931~942.
- 武显东,王宗起,罗金海,程家孝,闫全人,张英利,王师迪. 2014. 滇东北东川下田坝A型花岗岩锆石U-Pb年龄、地球化学特征及其构造意义. 地质通报,33(6):860~873.
- 肖加飞,魏家庸,胡瑞忠. 2004. 扬子地台西南缘早三叠世层序地层格架. 沉积学报,22(2):310~318.
- 熊国庆,江新胜,崔晓庄,卓皆文,陆俊泽,刘建辉,汪正江,王剑. 2013. 扬子西缘元古宙峨边群烂包坪组地层归属及其锆石SHRIMP U-Pb年代学证据. 地学前缘,20(4):350~360.
- 许连忠,张正伟,张乾,朱笑青,祝朝辉,黄艳,黄海明. 2006. 威宁宣威组底部硅质页岩Rb-Sr古混合线年龄及其地质意义. 矿物学报,26(4):387~394.
- 尹福光,孙志明,任光明,王冬兵. 2012b. 上扬子陆块西南缘早一中元古代造山运动的地质记录. 地质学报,86(12):1917~1932.
- 尹福光,孙志明,张璋. 2011. 会理—东川地区中元古代地层—构造格架. 地质论评,57(6):770~778.
- 尹福光,王冬兵,孙志明,任光明,庞维华. 2012a. 哥伦比亚超大陆在扬子陆块西缘的探秘. 沉积与特提斯地质,32(3):31~40.
- 张传恒,高林志,武振杰,史晓颖,闫全人,李大建. 2007. 滇中昆阳群凝灰岩锆石SHRIMP U-Pb年龄:华南格林威尔期造山的证据. 科学通报,52(7):818~824.
- 张远志. 1996. 云南省岩石地层. 武汉:中国地质大学出版社.
- 赵玉光,许效松,刘宝珺. 1996. 上扬子台地西缘峨眉地区三叠纪高频率层序与海平面振荡研究. 岩相古地理,16(1):1~18.
- 郑荣才,戴朝成,罗清林,汪小平,雷光明,蒋昊,陈虎. 2011. 四川类前陆盆地上三叠统须家河组沉积体系. 天然气工业,31(9):16~24.
- 周明忠,罗泰义,李正祥,赵辉,龙汉生,杨勇. 2008. 遵义牛蹄塘组底部凝灰岩锆石SHRIMP U-Pb年龄及其地质意义. 科学通报,53(1):104~110.
- 周明忠,罗泰义,刘世荣,钱志宽,邢乐才. 2013. 贵州江口平引老堡组顶部的锆石SHRIMP年龄与对比意义. 中国科学:地球科学,43(7):1195~1206.
- 朱江,张招崇,侯通,康健丽. 2011. 贵州盘县峨眉山玄武岩系顶部凝灰岩LA-ICP-MS锆石U-Pb年龄:对峨眉山大火成岩省与生 物大规模灭绝关系的约束. 岩石学报,27(9):2743~2751.
- 卓皆文,江新胜,王剑,崔晓庄,熊国庆,陆俊泽,刘建辉,马铭珠. 2013. 华南扬子古大陆西缘新元古代康滇裂谷盆地的开启时间与充填样式. 中国科学:地球科学,43(12):1952~1963.
- 卓皆文,汪正江,王剑,谢渊,杨平. 2009. 铜仁坝黄震旦系老堡组顶部晶屑凝灰岩SHRIMP锆石U-Pb年龄及其地质意义. 地质论评,55(5):639~646.
- Anderson T. 2002. Correction of common lead in U-Pb analyses that do not report 204Pb. Chemical Geology, 192: 59~79.
- Arai S. 1992. Chemistry of chromian spinel in volcanic rocks as a potential guide to magma chemistry. Mineralogical Magazine, 56: 173~184.
- Armstrong-Altrin J S, and Verma S P. 2005. Critical evaluation of six tectonic setting discrimination diagrams using geochemical data of Neogene sediments from known tectonic settings. Sedimentary Geology, 177: 115~129.
- Barnes S. J. and Roeder P L. 2001. The range of Spinel compositions in terrestrial mafic and ultramafic rocks. Journal of Petrology, 42: 2279~2302.
- Bhatia M R. 1983. Plate tectonic sand geochemical composition of sandstones. Journal of Geology, 91: 611~627.
- Chen Duofu, Dong Weiquan, Zhu Binquan, and Chen Xianpei. 2004. Pb-Pb ages of Neoproterozoic Doushantuo phosphorites in South China: constraints on early metazoan evolution and glaciation events. Precambrian Research, 132: 123~132.
- Chen Hongde, Zhang Chenggong, Huang Fuxi, Hou Mingcai. 2011&. Filling process and evolutionary model of sedimentary sequence of Middle—Upper Yangtze craton in Hercy—Indosinian (Devonian—Middle Triassic). Acta Petrologica Sinica, 27(8): 2281~2298.
- Chen Jiaxiao, Luo Jinhai, Wu Yudong, Han Kui, Wang Shidi. 2014&. Geochronology, geochemistry and tectonic significance of the Xiatianba granite in Northeastern Yunnan. Acta Geologica Sinica, 88(3): 337~346.
- Condon D, Zhu M Y, Bowring S, Wang W, Yang A H, and Jin Y G. 2005. U-Pb Ages from the Neoproterozoic Doushantuo Formation, China. Science, 308: 95~98.
- Cookenboo H O, Bustin R M, and Wilks K R. 1997. Detrital chromian spinel compositions used to reconstruct the tectonic setting of provenance; implications for orogeny in the Canadian Cordillera. Journal of Sedimentary Research, 67: 116~123.
- Deng B, Liu S G, Jansa L, Cao J X, Cheng Y, Li Z W, and Liu S. 2012. Sedimentary record of Late Triassic transpressional tectonics of the Longmenshan thrust belt, SW China. Journal of Asian Earth Sciences, 48: 43~55.
- Fan Weiming, Wang Yuejun, Peng Touping, Miao Laicheng, and Guo Feng. 2004. Ar-Ar and U-Pb geochronology of late Paleozoic basalts in western Guangxi and its constraint on the eruption age of Emeishan basalt magmatism. Chinese Science Bulletin, 49: 2318~2327.
- Fedo C M, Sircombe K N, and Rainbird R H. 2003. Detrital zircon analysis of the sedimentary record. Reviews in Mineralogy and Geochemistry, 53: 277~303.
- Gehrels G, Johnsson M J, and Howell D G. 1999. Detrital zircon geochronology of the Adams Argillite and Nation River Formation, East—Central Alaska, U. S. A. Journal of Sedimentary Research, 69: 135~144.
- Gehrels G. 2012. Detrital zircon U-Pb geochronology: Current methods and new opportunities. In: Busby C and Azor A. eds. Tectonics of

- sedimentary basins: Recent advances. John Wiley & Sons Ltd Publication, 47 ~ 62.
- González-Len C M, Valencia V A, Lawton T F, Amato J M, Gehrels G E, Leggett W J, Montijo-Contreras O, and Fernández M. 2009. The lower Mesozoic record of detrital zircon U-Pb geochronology of Sonora, Mexico, and its paleogeographic implications. *Revista Mexicana de Ciencias*, 26: 301 ~ 314.
- Greentree M R, Li Z X, Li X H, and Wu H C. 2006. Late Mesoproterozoic to earliest Neoproterozoic basin record of the Sibao orogenesis in western South China and relationship to the assembly of Rodinia. *Precambrian Research*, 151: 79 ~ 100.
- Gu Xueda, Liu Xiaohu. 1997#. Lithostratigraphy of Sichuan province. Wuhan: China University of Geosciences Press.
- He Bin, Xu Yigang, Xiao Long, Wang Kangming, Sha Shaoli. 2003&. Generation and spatial distribution of the Emeishan large igneous province: New evidence from stratigraphic records. *Acta Geologica Sinica*, 77(2): 194 ~ 202.
- Hou Kejun, Li Yanhe, Tian Yourong. 2009&. In situ U-Pb zircon dating using laser ablation-multi ion counting-ICP-MS. *Mineral Deposits*, 28(4): 481 ~ 492.
- Huang Fuxi, Chen Hongde, Hou Mingcai, Zhong Yijiang, Li Jie. 2011&. Filling process and evolutionary model of sedimentary sequence of Middle—Upper Yangtze craton in Caledonian (Cambrian—Silurian). *Acta Petrologica Sinica*, 27(8): 2299 ~ 2317.
- Jackson S E, Pearson N J, Griffin W L, and Belousova E A. 2004. The application of laser ablation-inductively coupled plasma-mass spectrometry to in situ U-Pb zircon geochronology. *Chemical Geology*, 211: 47 ~ 69.
- Jiang Xinsheng, Wang Jian, Cui Xiaozhuang, Zhuo Jiewen, Xiong Guoqing, Lu Junze, and Liu Jianhui. 2012. Zircon SHRIMP U-Pb geochronology of the Neoproterozoic Chengjiang Formation in central Yunnan Province (SW China) and its geological significance. *Science China Earth Sciences*, 55: 1815 ~ 1826.
- Jorge R C G S, Fernandes P, Rodrigues B, Pereira Z, and Oliveira J T. 2013. Geochemistry and provenance of the Carboniferous Baixo Alentejo Flysch Group, South Portuguese Zone. *Sedimentary Geology*, 284 ~ 285: 133 ~ 148.
- Kalsbeek F, Frei D, and Affaton P. 2008. Constraints on provenance, stratigraphic correlation and structural context of the Volta basin, Ghana, from detrital zircon geochronology: An Amazonian connection? *Sedimentary Geology*, 212: 86 ~ 95.
- Kamenetsky V S, Crawford A J, and Meffer S. 2001. Factors controlling chemistry of magmatic spinel: an empirical study of associated olivine, Cr-spinel and melt inclusions from primitive rocks. *Journal of Petrology*, 42: 655 ~ 671.
- Lee Y. 1999. Geotectonic significance of detrital chromian spinel: a review. *Geosciences Journal*, 3: 23 ~ 29.
- Leier A L, Kapp P, Gehrels G E, and Decelles P G. 2007. Detrital zircon geochronology of Carboniferous—Cretaceous strata in the Lhasa terrane, southern Tibet. *Basin Research*, 19: 361 ~ 378.
- Lenaz D, Kamenetsky V S, Crawford A J, and Princivalle F. 2000. Melt inclusions in detrital spinel from the SE Alps (Italy—Slovenia): a new approach to provenance studies of sedimentary basins. *Contributions to Mineralogy and Petrology*, 139: 748 ~ 758.
- Lenaz D, Mazzoli C, Spišiak J, Princivalle F, and Maritan L. 2009. Detrital Cr-spinel in the Šambron—Kamenica Zone (Slovakia): evidence for an ocean-spreading zone in the Northern Vardar suture? *International Journal of Earth Sciences*, 98: 345 ~ 355.
- Li Wenbo, Huang Zhilong, Zhang Guan. 2006&. Sources of the ore metals of the Huize ore field in Yunnan province: Constraints from Pb, S, C, H, O and Sr isotope geochemistry. *Acta Petrologica Sinica*, 22(10): 2567 ~ 2580.
- Li X H, Li Z X, Zhou H W, Liu, Y, and Kinny, P D. 2002. U-Pb zircon geochronology, geochemistry and Nd isotopic study of Neoproterozoic bimodal volcanic rocks in the Kangdian Rift of South China: implications for the initial rifting of Rodinia. *Precambrian Research*, 113: 135 ~ 154.
- Li Xianhua, Zhou Hanwen, Li Zhengxiang, Liu Ying. 2002&. Petrogenesis of Neoproterozoic bimodal volcanic in western Sichuan and its tectonic implications: Geochemical and Sm-Nd isotopic constraints. *Chinese Journal of Geology*, 37(3): 264 ~ 276.
- Lin Guangchun, Li Xianhua, Li Wuxian. 2007&. SHRIMP U-Pb zircon age, geochemistry and Nd—Hf isotope of Neoproterozoic mafic dyke swarms in western Sichuan: Petrogenesis and tectonic significance. *Science China Earth Sciences*, 50(1): 1 ~ 16.
- Lin Liangbiao, Chen Hongde, Jiang Ping, Hu Xiaoqiang, Ji Xiangtian, Ye Liming. 2006&. Sedimentary facies and litho—paleogeographic evolution of the upper Triassic Xujiahe Formation in West Sichuan foreland basin. *Journal of Chengdu University of Technology (Science & Technology Edition)*, 33(4): 376 ~ 383.
- Liu Yongsheng, Gao Shan, Hu Zhaochu, Gao Changgui, Zong Keqing, and Wang Dongbing. 2009. Continental and oceanic crust recycling-induced melt—peridotite interactions in the Trans-North China Orogen: U-Pb dating, Hf isotopes and trace elements in zircons from mantle xenoliths. *Journal of Petrology*, 51: 537 ~ 571.
- Ludwig K R. 2003. User's manual for Isoplot 3.0: Geochronological toolkit for Microsoft Excel. Berkeley Geochronology Center Special Publication, 4;1 ~ 70.
- Naipauer M, Vujovich G I, Cingolani C A, and McClelland W C. 2010. Detrital zircon analysis from the Neoproterozoic—Cambrian sedimentary cover (Cuyania terrane), Sierra de Pie de Palo, Argentina: Evidence of a rift and passive margin system? *Journal of South American Earth Sciences*, 29: 306 ~ 326. Nelson J, and Gehrels G. 2007. Detrital zircon geochronology and provenance of the southeastern Yukon—Tanana terran. *Canadian Journal of Earth Sciences*, 44: 297 ~ 316.
- Nemec W, and Steel R J. 1984. Alluvial and coastal conglomerates: their significance features and some comments on gravelly mass-flow deposits. *Canadian Society of Petroleum Geologists Memoir*, 10: 1 ~ 31.
- Paktunc A D, and Cabri L J. 1995. A proton- and electron-microprobe study of gallium, nickel and zinc distribution in chromian spinel. *Lithos*, 35: 261 ~ 282.
- Ren Guangming, Pang Weihua, Sun Zhiming, Yin Fuguang, Xiao Qiliang. 2013&. Zircon U-Pb geochronology and geochemistry of mafic dyke swarms in Dengxiangying Group on west margin of Yangtze Block, China. *Journal of Chengdu University of Technology (Science & Technology Edition)*, 40(1): 66 ~ 79.
- Roser B P, and Korsch R J. 1988. Provenance signatures of sandstone—mudstone suites determined using discriminant function analysis of major-element data. *Chemical Geology*, 67: 119 ~ 139.
- Ryan K M, and Williams D M. 2007. Testing the reliability of discrimination diagrams for determining the tectonic depositional environment of ancient sedimentary basins. *Chemical Geology*, 242: 103 ~ 125.

- Sawaki Y, Nishizawa M, Suo T, Komiya T, Hirata T, Takahata N, Sano Y, Han J, Kon Y, and Maruyama S. 2008. Internal structures and U-Pb ages of zircons from a tuff layer in the Meishucunian formation, Yunnan Province, South China. *Gondwana Research* 14: 148 ~ 158.
- Shao Longyi, Gao Caixia, Zhang Chao, Wang Hao, Guo Lijun, Gao Caihong. 2013&. Sequence—Palaeogeography and coal accumulation of Late Permian in Southwestern China. *Acta Sedimentologica Sinica*, 31(5): 856 ~ 866.
- Shellnutt J G, Zhou M F, Yan D P, and Wang Y B. 2008. Longevity of the Permian Emeishan mantle plume (SW China): 1 Ma, 8 Ma or 18 Ma? *Geological Magazine* 145: 373 ~ 388.
- Shi Zhiqiang, Yin Haisheng, Zeng Deyong, Zhang Hua. 2010&. The lowest member of Lower Triassic Feixianguan Formation in Upper Yangtze region: Sedimentary records from sluggish water to turbulent ocean after the mass extinction. *Geological Review*, 56(6): 769 ~ 780.
- Sirccombe K N. 1999. Tracing provenance through the isotope ages of littoral and sedimentary detrital zircon, eastern Australia. *Sedimentary Geology*, 124: 47 ~ 67.
- Tang Yong, Qin Jianxiong. 2007&. Research on Triassic sedimentary environment in the Xichang Basin, Sichuan. *Acta Geologica Sichuan*, 27(2): 92 ~ 95.
- Tian Jingchun, Chen Hongde, Peng Jun, Qin Jianxiong, Hou Zhongjian, Shou Jianfeng, Yang Xiaoning, Shen Anjiang, Chen Ziliao. 2000&. Sequence division, correlation and framework of Lower and Middle Triassic in Sichuan—Guizhou—Yunnan—Guangxi region. *Acta Sedimentologica Sinica*, 18(2): 198 ~ 204.
- Wang Dongbing, Sun Zhiming, Yin Fuming, Wang Liqian, Wang Baodi, Zhang Wanping. 2012&. Geochronology of the Hekou Group on the western margin of the Yangtze Block: Evidence from zircon LA-ICP-MS U-Pb dating of volcanic rocks. *Journal of Stratigraphy*, 36(3): 630 ~ 635.
- Wang Dongbing, Yin Fuming, Sun Zhiming, Wang Liqian, Wang Baodi, Liao Shiyong, Tang Yuan, Ren Guangming. 2013&. Zircon U-Pb age and Hf isotope of Paleoproterozoic mafic intrusion on the western margin of the Yangtze Block and their implications. *Geological Bulletin of China*, 32(4): 617 ~ 630.
- Wang Jian, Liu Baojun, Pan Guitang. 2001&. Neoproterozoic rifting history of South China significance to Rodinia breakup. *Journal of Mineralogy and Petrology*, 21(3): 135 ~ 145.
- Wang Zizheng, Guo Yang, Yang Bin, Wang Shengwei, Sun Xiaoming, Hou Lin, Zhou Bangguo, Liao Zhenwen. 2013&. Geochemistry and zircon U-Pb dating of Tangtang granite in the western margin of the Yangtze Platform. *Acta Geologica Sinica*, 87(7): 931 ~ 942.
- Wu Yudong, Wang Zongqi, Luo Jinhai, Cheng Jiaxiao, Yan Quanren, Zhang Yingli, Wang Shidi. 2014&. LA-ICP-MS zircon U-Pb age and geochemistry of Xiatianba A-type granites in Dongchuan, Northeast Yunnan, and their tectonic significance. *Geological Bulletin of China*, 33(6): 860 ~ 873.
- Xiao Jiafei, Wei Jiayong, Hu Ruizhong. 2004&. The Early Triassic sequence stratigraphic framework in southwestern margin of Yangtze platform. *Acta Sedimentologica Sinica*, 22(2): 310 ~ 318.
- Xiong Guoqing, Jiang Xinsheng, Cui Xiaozhuang, Zhuo Jiewen, Lu Junze, Liu Jianhui, Wang Zhengjiang, Wang Jian. 2013&. Strata location of the Lanbaoping Formation of the Proterozoic Ebian Group in the Western Yangtze Block and its chronological evidence of zircon SHRIMP U-Pb age. *Earth Science Frontiers*, 20(4): 350 ~ 360.
- Xu Lianzhong, Zhang Zhengwei, Zhang Qian, Zhu Xiaoqing, Zhu Chaohui, Huang Yan, Huang Haiming. 2006&. The age of siliceous shale in the lower part of the Xuanwei Formation in Weining and its geological implications. *Acta Mineralogica Sinica*, 26(4): 387 ~ 394.
- Xu Y G, Chung S L, Jahn B M, Wu G Y. 2001. Petrologic and geochemical constraints on the petrogenesis of Permian—Triassic Emeishan flood basalts in southwestern China. *Lithos*, 58: 145 ~ 168.
- Xu Y G, He B, Chung S-L, Menzies M A, and Frey F A. 2004. Geologic, geochemical, and geophysical consequences of plume involvement in the Emeishan flood-basalt province. *Geology*, 32: 917 ~ 920.
- Xu Yigang, Luo Zhenyu, Huang Xiaolong, He Bin, Xiao Long, Xie Liewen, and Shi Yuruo. 2008. Zircon U-Pb and Hf isotope constraints on crustal melting associated with the Emeishan mantle plume. *Geochimica et Cosmochimica Acta*, 72: 3084 ~ 3104.
- Yin Fuguang, Sun Zhiming, Ren Guangming, Wang Dongbing. 2012b&. Geological record of Paleo- and Mesoproterozoic orogenesis in the western margin of Upper Yangtze Block. *Acta Geologica Sinica*, 86(12): 1917 ~ 1932.
- Yin Fuguang, Sun Zhiming, Zhang Zhang. 2011&. Mesoproterozoic stratigraphic—structure framework in Huili—Dongchuan area. *Geological Review*, 57(6): 770 ~ 778.
- Yin Fuguang, Wang Dongbing, Sun Zhiming, Ren Guangming, Pang Xionghua. 2012a&. Columbia supercontinent: New insights from the western margin of the Yangtze landmass. *Sedimentary Geology and Tethyan Geology*, 32(3): 31 ~ 40.
- Zhang Chuanheng, Gao Linzhi, Wu Zhenjie, Shi Xiaoying, Yan Quanren, Li Dajian. 2007&. SHRIMP U-Pb zircon age of tuff from the Kunyang Group in central Yunnan: Evidence for Grenvillian orogeny in South China. *Chinese Science Bulletin*, 52(11): 1517 ~ 1525.
- Zhang Zhiyuan. 1996#. Lithostratigraphy of Yunnan province. Wuhan: China University of Geosciences Press.
- Zhao Junhong, and Zhou Meifu. 2007. Geochemistry of Neoproterozoic mafic intrusions in the Panzhihua district (Sichuan Province, SW China): Implications for subduction-related metasomatism in the upper mantle. *Precambrian Research*, 152: 27 ~ 47.
- Zhao Xinfu, Zhou Meifu, Li Jianwei, Sun Min, Gao Jianfeng, Sun Weihua, and Yang Jinhui. 2010. Late Paleoproterozoic to early Mesoproterozoic Dongchuan Group in Yunnan, SW China: Implications for tectonic evolution of the Yangtze Block. *Precambrian Research*, 182: 57 ~ 69.
- Zhao Yuguang, Xu Xiaosong, Liu Baojun. 1996&. High-frequency sequences and sea-level oscillations in the Emei area on the western margin of the upper Yangtze platform. *Journal of Palaeogeography*, 16(1): 1 ~ 18.
- Zheng Rongcui, Dai Chaocheng, Luo Qinglin, Wang Xiaoping, Lei Guangming, Jiang Hao, Chen Hu. 2011&. Sedimentary system of the Upper Triassic Xujiahe Formation in the Sichuan foreland basin. *Natural Gas Industry*, 31(9): 16 ~ 24.
- Zhong Hong, Zhu Weiguang, Chu Zhuyin, He Defeng, and Song Xieyan. 2007. SHRIMP U-Pb zircon geochronology, geochemistry, and Nd—Sr isotopic study of contrasting granites in the Emeishan large igneous province, SW China. *Chemical Geology*, 236: 112 ~ 133.

Zhou Mingzhong, Luo Taiyi, Li Zhengxiang, Zhao Hui, Long Hansheng, Yang Yong. 2008&. SHRIMP U-Pb zircon age of tuff at the bottom of the Lower Cambrian Niutitang Formation, Zunyi, South China. Chinese Science Bulletin, 53(4): 576~583.

Zhou Mingzhong, Luo Taiyi, Liu Shirong, Qian Zhikuan, Xing Lecai. 2013&. SHRIMP zircon age for a K-bentonite in the top of the Laobao Formation at the Pingyin section, Guizhou, South China. Science China Earth Sciences, 56(10): 1677~1687.

Zhu Jiang, Zhang Zhaochong, Hou Tong, Kang Jianli. 2011&. LA-ICP-MS zircon U-Pb geochronology of the tuffs on the uppermost of the Emeishan basalt succession in Panxian County, Guizhou: Constraints on genetic link between Emeishan large igneous province

and the mass extinction. Acta Petrologica Sinica, 27(9): 2743~2751.

Zhuo Jiewen, Wang Xinsheng, Wang Jian, Cui Xiaozhuang, Xiong Guoqing, Lu Junze, Liu Jianhui, Ma Mingzhu. 2013&. Opening time and filling pattern of the Neoproterozoic Kangdian Rift Basin, western Yangtze Continent, South China. Science China Earth Sciences, 56(10): 1664~1676.

Zhuo Jiewen, Wang Zhengjiang, Wang Jian, Xie Yuan, Yang Ping. 2009&. SHRIMP zircon U-Pb age of crystal tuffs on the top of Sinian Laobao Formation at Bahuang, Tongren area, and its geological implications. Geological Review, 55(5): 639~646.

Chromian Spinel, Zircon Age Constraints on the Provenance of Early Triassic Feixianguan Formation Sandstones from Huize Area, Upper Yangtze Region

ZHANG Yingli¹⁾, WANG Zongqi¹⁾, WANG Gang¹⁾, LI Qian²⁾, LIN Jianfei³⁾

- 1) MLR Key Laboratory of Metallogeny and Mineral Assessment, Institute of Mineral Resources, CAGS, Beijing, 100037;
- 2) Research Institute of Petroleum Exploration & Development, PetroChina, 100083;
- 3) University of Geosciences (Beijing), Beijing, 100083

Objectives: Huize area is situated between the Kandian Oldland and Sichuan basin with well-preserved sedimentary records. Achievements were mainly on sedimentary environments and lithofacies palaeogeography of the Feixianguan Formation. Its provenance and tectonic setting are not well understood. Based on sedimentary successions, we focus on the heavy mineral analysis to evaluate their sources.

Methods: Heavy mineral fractions from approximately 10 kg sample No. 10HLS2 and 10HLS16 of siliciclastic rock were concentrated and separated into 100, 150 and 250 μm size fractions by standard techniques of density and magnetic separation at the Langfang Institute of Regional Geological and Mineral Resource Survey, Hebei Province, China. Detrital heavy minerals (chromian spinel and zircon) were separated from sample No. 10HLS2 for electron probe microanalysis (EPMA) and LA-ICP-MS U-Pb dating.

Two mineral fractions above of roughly 300 grains were randomly handpicked in alcohol under a binocular microscope, mounted in epoxy along with known standards, and polished to expose grain centers for backscattered electron (BSE) imaging and EPMA analysis. Distinct domains within the heavy minerals were selected for analysis based on the BSE images.

Determination of the major element compositions of detrital chromian spinel was performed by wavelength-dispersive spectrometry using an EPMA-1600 electron probe microanalyzer at the China University of Geoscience (Beijing). The operating conditions were: accelerating voltage 15kV, beam current 10 nA and beam diameter 1 μm . We used as standars: magnetite (Fe), albite (Si, Na, Al), apatite (Ca, P), rutile (Ti), rhodonite (Mn), sanidine (K), olivine (Mg), fluorite (F), monazite (La, Ce, Pr, Nd, Th), zircon (Y, Zr, Hf), pollucite (Rb, Cs) and single mineral (U, Ta, Nb). The calculation are based on the CALCMIN excel program.

Results: Feixianguan Formation is mainly purple red fluvial sandstone in Huize area, Upper Yangtze. Sediments were demonstrated to have mainly come from west and northwestern margin as indicated by restored paleo-current directions. Heavy mineral assemblages indicate that the provenance was mainly from igneous rocks, which significant amounts of detrital Cr-spinels and zircon were observed. Electron microprobe results show that those detrital spinels are characterized by high Cr, low Fe^{3+} and high TiO_2 concentrations, which indicates sources of volcanic related to ocean island/intraplate, island arc and Large Igneous Province. Meanwhile, detrital zircon

LA-ICP-MS U-Pb dating shows that the sources of Feixianguan Formation were mainly from the 248 ~ 272 Ma and 548 ~ 997 Ma magmatic rocks. **Conclusions:** Comprehensive analysis of chromian spinel and detrital zircons suggest that 248 ~ 272 Ma rocks featured with large igneous province basalts were mainly derived from the Emei Mountain basalt and the same basic intrusive rocks, and 715 ~ 997 Ma rocks with ocean island / within plate basalts were mainly sourced from Neoproterozoic Suxiong Formation and the same period magmatic rocks. 1000 ~ 1100 Ma rocks forming in island arc indicated by chromian spinels also provided some sediment. Furtherly, detrital zircon dating also shows that there occurred magmatism in the Paleoproterozoic and Early Cambrian on the western margin of Yangtze block area. There also exists Neoarchean crystallization basement. All of these provided evidences about tectonic evolution in the upper Yangtze Region.

Keywords: Upper Yangtze region; detrital heavy minerals; chromian spinel; detrital zircon geochronology; provenance analysis.

Acknowledgements: This study was financially supported by the Natural Science Foundation of China (No. 41302080) and Chinese Geological Survey (No. 12120114009401). We would like to express our thanks to Hao Jinhua from China University of Geosciences (Beijing) for electron microprobe analysis. We are also indebted to Doctor Hou Kejun from the Institute of Mineral Resources, Chinese Academy of Geological Sciences for isotopic dating.

First author: ZHANG Yingli, male, born in 1979, assistant research fellow. Mainly engaged in sedimentology and basin tectonics. Address: No. 26, Baiwanzhuang Street, Xicheng District, Beijing, 100037. Email: yinglizh@126.com.

Manuscript received on: 2014-09-14; Accepted on: 2015-10-10; Edited by: HUANG Min.

Doi: 10.16509/j.georeview.2016.01.005

《地质论评》等蝉联“中国最具国际影响力学术期刊”

2015年12月18~19日,在中国期刊协会、中国科学技术期刊编辑学会、中国高校科技期刊研究会、全国高等学校文科学报研究会、中国学术期刊(光盘版)电子杂志社有限公司等主办的“中国学术期刊未来论坛”上,中国学术期刊(光盘版)电子杂志社有限公司等揭晓了“2015中国最具国际影响力学术期刊”和“2015中国国际影响力优秀学术期刊”。由中国地质学会主办的*Acta Geologica Sinica (English Edition)*、《地质学报》、《地质论评》、《矿床地质》和《岩石矿物学杂志》均在2012年以来连续4年获得“中国国际影响力优秀学术期刊”称号。

中国知网统计了我国6100多种学术期刊被WOS期刊(美国汤森路透公司科学引文数据库总称,包括SCI、SSCI、A&HCI及会议论文集)的总被引频次、他引总被引频次、影响因子等计量指标,按一定公式计算了各期刊的国际影响力指数,进而遴选出“中国最具国际影响力学术期刊”(前5%,其中自然科学与工程技术类期刊175种,人文社会科学类期刊60种)和“中国国际影响力优秀学术期刊”(前5%~10%)。

2015年,《地质学报》(英文版)国际影

响力指数是216.250名,排名第28位;《地质学报》(中文版)国际影响力指数是182.890名,排名第36位;《地质论评》国际影响力指数是87.185名,排名第114位。

